AN ABSTRACT OF THE THESIS OF

Nathan E. Casebeer for the degree of Master of Science in Geology presented on November 12, 2004.

Title: Sediment Storage in a Headwater Valley of the Oregon Coast Range: Erosion Rates and Styles and Valley-Floor Capacitance.

Abstract approved: _____

Stephen T. Lancaster

This study is part of the effort to quantify sediment budgets and understand the geomorphic evolution of steep mountains where debris flows are the dominant agent of upland erosion. Observations indicate that headwater basins in the Oregon Coast Range (OCR) can store a large amount of sediment, mostly from debris flows, in wide valley floors. In Bear Creek, a 2.23 km^2 tributary basin of Knowles Creek, surveyed sediment volume in the main-stem valley was 6.95×10^4 m^3. We hypothesize that, by storing sediment, headwater valleys in the OCR act as a sediment reservoir that buffers larger-basin reaches from episodic debris flows. These reservoirs are "well-mixed": they release sediment "cohorts" in proportion to their relative volumes in storage and, therefore, have an exponential distribution of sediment ages or residence times. This exponential distribution of residence times results from these valleys receiving pulse inputs of sediment at discrete times and producing gradual outputs of sediment representing a wide range of input times. We determined two separate residence time distributions in Bear Creek by dividing the main-stem valley into two reservoirs: lower and upper reaches. In each of these reaches, wood and/or charcoal from randomly selected sampling points in the valley sediment were dated by radiocarbon methods. The mean radiocarbon age from sediments in the upper-reach was 4.43×10^2 years. The mean radiocarbon age from sediments in the lower-reach was 1.22×10^3 years. The volume-weighted mean age of sediments in the entire main-stem valley was 9.96×10^2 years. Erosion rates of 0.013 - 0.038 mm/yr and 0.011 - 0.033

mm/yr for each of the upper 1.32 km^2 and full 2.23 km^2 basins, respectively, were calculated by dividing the volume of sediment by the mean age and the contributing area. A density correction for conversion of rock to sediment defines the lower limit with no density change defining the upper limit. These erosion rates are generally lower than those determined by other methods in the OCR possibly reflecting inherited age in radiocarbon dates plus denudation by processes that do not form deposits datable by radiocarbon. Such denudation processes include dissolution of bedrock and sediments and the direct discharging of soil from the hillslopes to the channel, transported as suspended load. In order to account for inherited radiocarbon ages and assuming that all denudation processes cycle sediment through the reservoirs datable by radiocarbon, we re-scaled the residence time distributions using independently derived mean ages for the sediment. These mean residence times are 5.5×10^1 years for the upper-reach and 1.18×10^2 years for the lower-reach, respectively. These mean residence times are derived from an assumed basin average erosion rate of 0.1 mm/yr. A two-stage δ-corrected Kolmogorov-Smirnov statistical goodness-of-fit test was used to find whether the radiocarbon age distributions from the upper and lower reaches are statistically consistent with exponential distributions defined by the mean sediment ages in each reach and, thus the hypothesis that these valley floors act as well mixed reservoirs. At the 5% significance level the lower-reach ages are consistent with an exponential distribution while the upper-reach ages are not. Combined with geomorphic and stratigraphic data, these statistical results support the conclusion that the lower-reach acts as a well mixed reservoir for episodic debris flows that form deposits that are then randomly and incrementally removed by fluvial reworking. Deviations in the shape of upper-reach's distribution from exponential may reflect a lesser degree of mixing as determined from geomorphic and stratigraphic data and also limitations in the determination of residence times. The upper-reach has less sediment than the lower-reach and a greater proportion of that are too young to reliably date by radiocarbon methods.

Sediment Storage in a Headwater Valley of the Oregon Coast Range: Erosion Rates and Styles and Valley-Floor Capacitance

by
Nathan E. Casebeer

A THESIS

submitted to

Oregon State University

in partial fulfillment of
the requirements for the
degree of

Master of Science

Presented November 12, 2004
Commencement June 2005

Master of Science thesis of Nathan E. Casebeer

Presented on November 12, 2004.

APPROVED:

Major Professor, representing Geology

Chair of the Department of Geosciences

Dean of the Graduate School

I understand that my thesis will become part of the permanent collection of Oregon State University libraries. My signature below authorizes release of my thesis to any reader upon request.

Nathan E. Casebeer, Author

ACKNOWLEDGEMENTS

The author expresses sincere appreciation to all those who made this thesis possible. Stephen Lancaster, my advisor, provided extensive support and was always available for help throughout the course of the project. Gordon Grant and Andrew Meigs provided reviews and discussions that yield useful insight. I sought and received useful advice on methods from Grant Meyer, Karl Wegmann, Cliff Riebe, and Ed Brook. Finally, Gordon Grant provided a summer of funding that helped make this project possible.

TABLE OF CONTENTS

LIST OF FIGURES

LIST OF FIGURES (Continued)

LIST OF TABLES

Sediment Storage in a Headwater Valley of the Oregon Coast Range: Erosion Rates and Styles and Valley-Floor Capacitance.

INTRODUCTION

Sediment dynamics and the interaction between sediment transport and bedrock erosion are difficult to characterize in landscapes (Sklar and Dietrich, 1998, 2000; Whipple and Tucker, 2002). Landscape evolution models commonly treat the fluvial system in mountain basins as sufficiently competent to transport all sediment delivered to it from hillslopes and river erosion, i.e. detachment-limited (Tucker and Bras, 1998; Whipple and Tucker, 2002). Although this assumption may work on geologic timescales for bedrock reaches with large water discharges, it becomes tenuous in steeper drainages (channel slopes greater than ~0.03 to 0.10) with smaller flows and on shorter timescales. In steeper drainages, which may comprise greater than 80% of the length of large unglaciated mountain basins, erosion is commonly dominated by episodic events of mass wasting (Benda and Dunne, 1997a; Kirchner et al. 2001; Stock and Dietrich, 2003). These events are shallow (~1—4 m), translational failures, or landslides of slope material, soil or colluvium. Colluvium is material deposited by mass-movement process including soil creep and debris flows. These landslides, usually within seconds, become debris flows (Iverson et al., 1997; Iverson et al., 2000; Reid et al., 1997), which are rapid (e.g., velocity ~ 10 m/s), liquefied flows of mixtures of water, sediment, and in the Pacific Northwest, wood and usually entrain additional material during runout both downslope and downstream. In many mountain landscapes mass wasting provides more sediment than the streams carry on shorter timescales, and the rates of deposition by mass wasting in headwater valleys are poorly known (Dietrich and Dunne, 1978; Benda and Dunne, 1997b; Lancaster et al., 2001).

How do fluvial systems respond to periodic inundation of their upper reaches by sediment yet continue to erode bedrock in uplifting terrain? How is

sediment delivered by mass wasting transferred downstream? Little is known about how aggradation and erosion interact with the construction and lateral erosion of valley floor surfaces to govern sediment transport through the system (Lisle and Church, 2002; Richards, 2002). In valley reaches dominated by debris-flow scour, subsequent larger, but rare, events may remove the deposits of smaller debris flows and scour the underlying bedrock (Miller and Benda, 2000). In valley reaches where debris flows deposit but bedrock erosion is primarily fluvial, incision may be accompanied by a strong component of lateral erosion in response to the excess sediment load (Hancock and Anderson, 2002). This study seeks to characterize and distinguish among the styles of sediment transport present in a headwater valley of the Oregon Coast Range. Understanding how this part of the landscape modulates the sediment flux through the valley network is important in both stratigraphic and geomorphic interpretations of climatic or tectonic forcing.

In the Oregon Coast Range, a debris-flow—dominated landscape, long-term (10^3 yr) erosion rates and short-term (10^1 yr) fluvial sediment yields are approximately equal (Dietrich and Dunne, 1978; Reneau and Dietrich, 1991; Heimsath et al. 2001). This result contrasts with other landscapes dominated by mass wasting, such as the mountains of central Idaho. In central Idaho, long-term erosion rates constrained by cosmogenic ^{10}Be (10^3 yr) and apatite fission tracks (10^6 yr) are, on average, 17 times higher than indicated by stream sediment yields measured over 10-84 years (Kirchner et al. 2001). This 17-fold discrepancy indicates that over geologic time scales, major episodic erosional events including mass wasting are responsible for most erosion. No such discrepancy characterizes the Oregon Coast Range. Here, field data and modeling efforts suggests that much of the sediment delivered to the drainage network is temporarily stored in fans and headwater valley floors rather than immediately contributing to the sediment yield of larger streams (Lancaster et al. 2001). In particular, woody

debris may increase the storage capacity of these valley floors (Lancaster et al. 2001) and force alluvial deposition by damming the channel (Montgomery et al., 2003). In effect, the headwater system buffers the sediment supply to larger streams. Thus, short-term sediment yields are approximately equal to the long-term sediment supply because the sediments from episodic erosional events are stored in the headwaters and released incrementally by fluvial erosion.

In a 2.1 km^2 tributary of Hoffman Creek, in the Oregon Coast Range, Lancaster et al. (2001) measured a volume of 9.32×10^4 m^3 of sediment stored in wide valley cross-sections. Similarly, other ~2 km^2 tributary valleys of the Siuslaw Basin were measured (Lancaster unpublished data, 2000) and shown to have wide valley floors relative to channel widths that provide accommodation space for sediment storage (Figures 1 and 3). Observations suggest that sediment inundation by debris flows forces lateral channel migration within the valley.

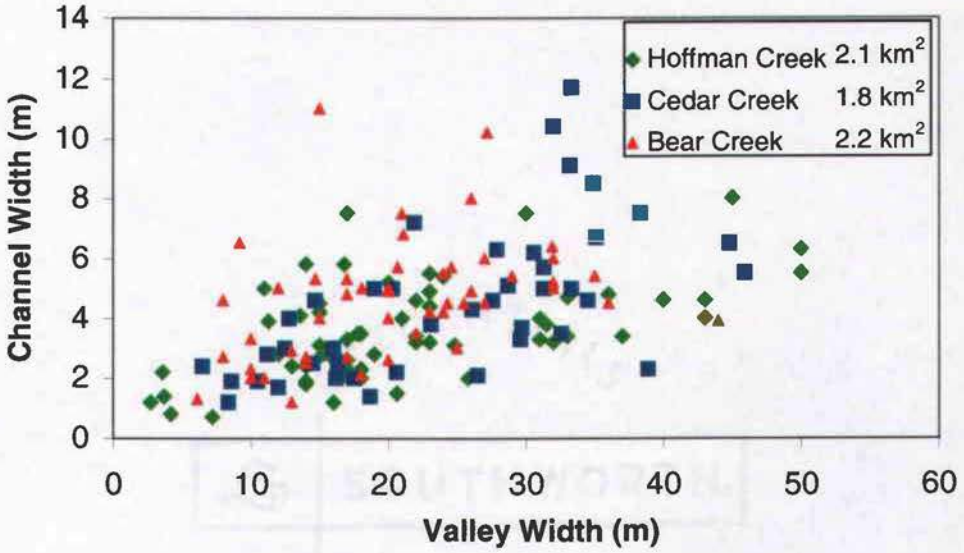

Figure 1. Wide valley floors relative to the channel widths provide sediment storage space in basins with ~2 km^2 drainage areas.

Large woody debris may block the channel and cause migration as well. Of these three measured valley reaches, two have little exposed bedrock, and the depth and volume of the sediment are not well known. In these basins, it is inferred that underlying the wide valley floor sediment is a similarly wide, horizontal bedrock surface, or strath. A strath terrace is commonly referred to as an abandoned bedrock surface overlain by sediment (e.g. Personius et al., 1993; Hancock and Anderson, 2002; Wegmann and Pazzaglia, 2002). Here, the definition of strath is broadened to include an "actively" forming bedrock surface overlain by sediment. The inference of actively forming straths in these measured basins is supported by observation in one of the valleys, of a well-exposed, flat bedrock channel bed. From these observations, it is speculated that debris flow-triggered channel migration bevels straths by lateral planation and widens valley floors to accommodate the volume of sediment in storage over time. Widespread strath formation in response to regional stream aggradation has been documented for the Pleistocene-Holocene transition in the Oregon Coast Range (Personius et al., 1993). Similarly, present-day debris-flow aggradation and the response of the channel to migrate may widen valley floors to accommodate the episodic sediment supply and release it gradually by fluvial reworking. Regardless of the mechanisms that form and maintain the presently observed strath surfaces, it is hypothesized that this capacity for storage of sediment or accommodation space modulates the episodic debris flow sediment input to produce a less episodic fluvial sediment output. A prediction of this hypothesis is that the sediment in these valleys has a range of residence times that are consistent with an exponential distribution. This exponential distribution of residence times results from a valley behaving as if it were a fully mixed reservoir. "Mixing" in this sense results from the valley receiving pulse inputs of sediment at discrete times and producing gradual outputs of sediment representing a wide range of input

times due to the channel position that crosses through a wide-age range of deposits (Figure 2).

To test the hypothesis that sediment storage serves as a buffer or equivalently a capacitor to episodic mass wasting events by acting as a fully mixed reservoir, this study attempts to answer and explore the implications of the following questions. (1) What does the distribution of sediment ages, determined from radiocarbon dating of wood and/or charcoal uniformly sampled within the valley fill, tell us about the sediment "reservoir" represented by headwater valleys? (2) What are the characteristics of the reservoir, and what is its role in the sediment budget?

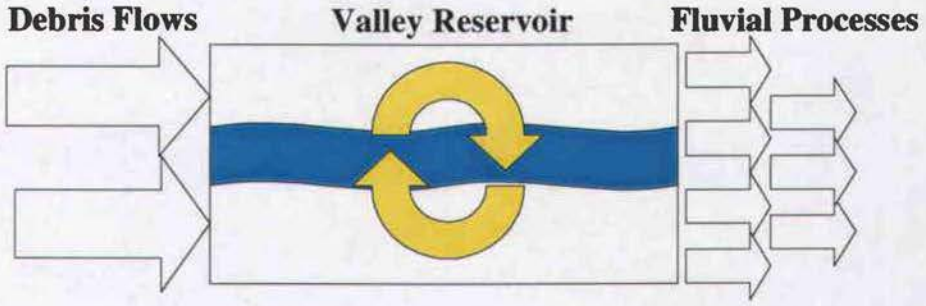

Figure 2. Schematic of valley sediment storage behaving as a fully mixed reservoir. The reservoir receives pulse inputs of sediment at discrete times (i.e. Debris Flows) and produces a gradual output representing a wide range of input times (Fluvial Processes). The reservoir behaves as if it were fully mixed due to the channel position that can remove a wide range of deposit ages.

STUDY AREA IN THE OREGON COAST RANGE

To address the hypothesis, a field study was conducted in Bear Creek, a 2.23 km^2 tributary basin of Knowles Creek (Figure 3). Bear Creek was suitable for this study because the channel runs over bedrock for much of its length and thus provides access to the full depth of the valley floor deposits in most places. This accessibility allowed for robust sediment volume estimates and radiocarbon dating of channel bank exposures (discussed below). Similar size basins in nearby Hoffman Creek (Lancaster et al., 2001, 2003) and elsewhere (Lancaster, unpublished data, 2000) have little exposed bedrock in the channel presumably due to recent disturbances (fires and timber harvesting) that have increased the recent debris-flow frequency and inundated the valleys. The Bear Creek basin,

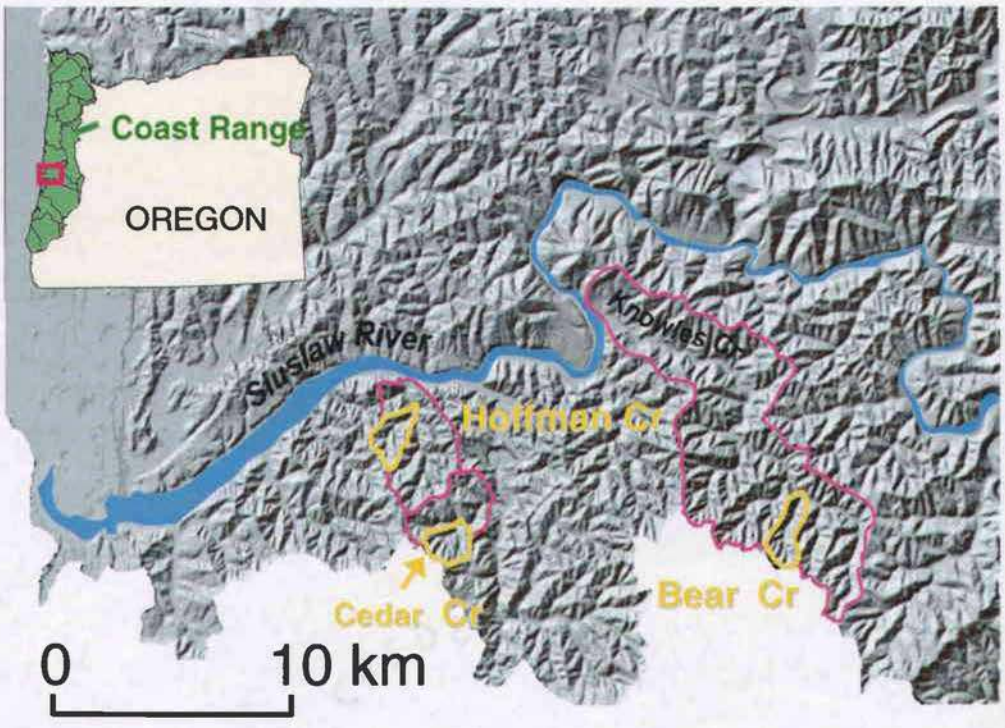

Figure 3. Location map of study basins in Hoffman Creek, Cedar Creek and Bear Creek (in Knowles Creek) outlined in yellow.

like the others mentioned, has homogeneous bedrock lithology; has no mid-slope or valley-bottom roads; is accessible; has available land-use records; and has occurrence of recent debris flows. The basins are underlain by massive, shallowly dipping, Eocene sandstone of the Tyee formation. Steep topography is characterized by 40° valley side-slopes and is highly dissected (Reneau and Dietrich, 1991). The high drainage density indicates the absence of deep-seated bedrock landslides in these basins that would erase the effects of fluvial and debris flow scour channel incision. Roering et al. (in press) confirmed this inference using automated topographic identification of deep-seated bedrock landslides in the Tyee Formation of the OCR. The maritime climate has warm, dry summers and mild, wet winters with a mean annual precipitation of approximately 1800 mm (Oregon Climate Service).

METHODS

Sediment Volumes

Surveyed sediment storage in Bear Creek provided a map for the selection of radiocarbon sampling locations (discussed below). Sediment volume was determined by calculating the cross-sectional area of the valley deposits at points along the main channel (as in Lancaster et al. 2001). The longitudinal profile of the main channel of the study basin was surveyed with a hand level and stadia rod. At intervals of about 10 channel widths, the geometry of valley transects were surveyed. Using the assumption that 40° valley sideslopes continue at depth below deposits, the cross-sectional area of sediment stored above the elevation of the channel was calculated. Combined with the channel survey, this information provided the sediment stored in the valley above the channel. Since much of the channel within Bear Creek exposes bedrock, this sediment storage is equal to the valley floor storage above bedrock. In a few locations, the valley floor deposits form distinct wedges, i.e., relatively flat surfaces followed by downward steps. Cross-sectional areas within wedges were estimated by connecting a line beneath the wedge in bedrock exposures upstream and downstream of the wedge (Figure 4). The cross-sectional area of the valley floor deposits as a function of distance from the outlet and longitudinal channel profile are shown in Figure 5.

Stratigraphic columns were measured in the channel banks at the locations of valley transects (Figure 6). These columns detailed the height of the banks and thickness of distinct units defined as coarse fluvial gravels, fluvially deposited fines, and debris flow deposits along the main-stem channel including debris fans entering the main-stem from tributaries. The bases of these columns are at the sediment-bedrock interface except for where sediment covers the channel bed. In such cases, the sediment cover is included in the total height of the channel banks.

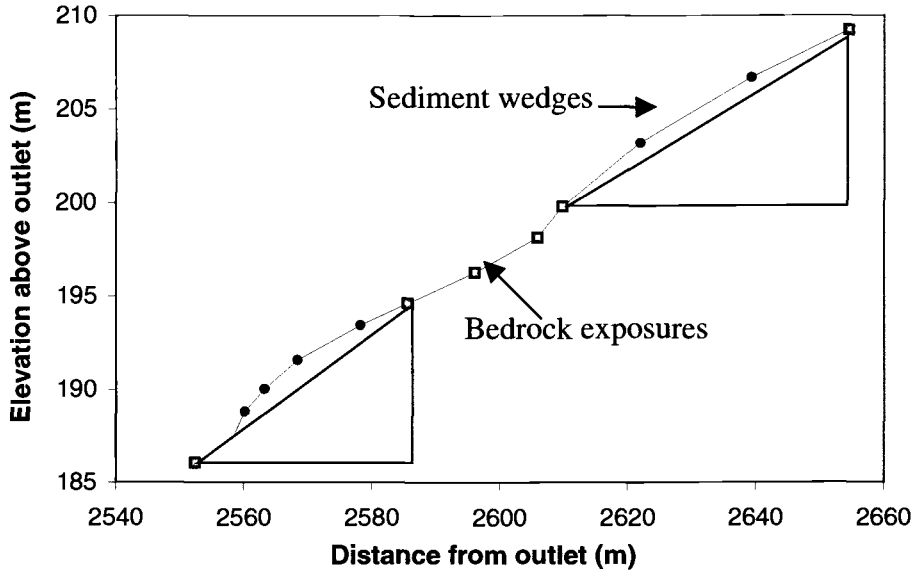

Figure 4. The cross-sectional areas of sediment wedges along the longitudinal channel profile were estimated by connecting a line beneath the wedge in bedrock exposures upstream and downstream of the wedge.

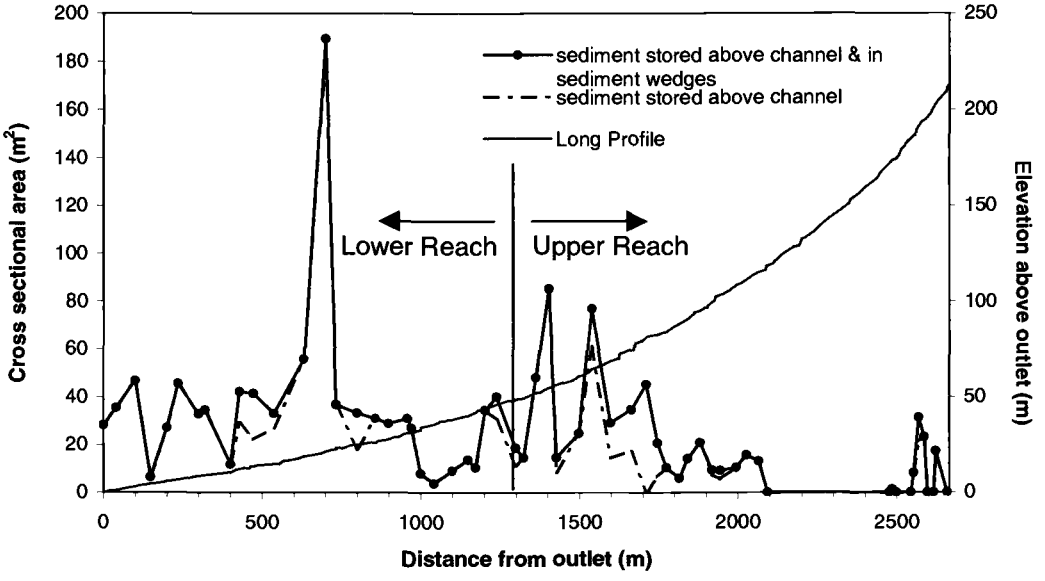

Figure 5. Surveyed Bear Creek channel profile with cross-sectional areas of sediment stored in surveyed valley transects as a function of distance from the outlet. Two storage estimates are shown: sediment stored above the channel bed, representing a minimum estimate; and a more realistic estimate including sediment wedges. Designations of Lower Reach and Upper Reach are explained below.

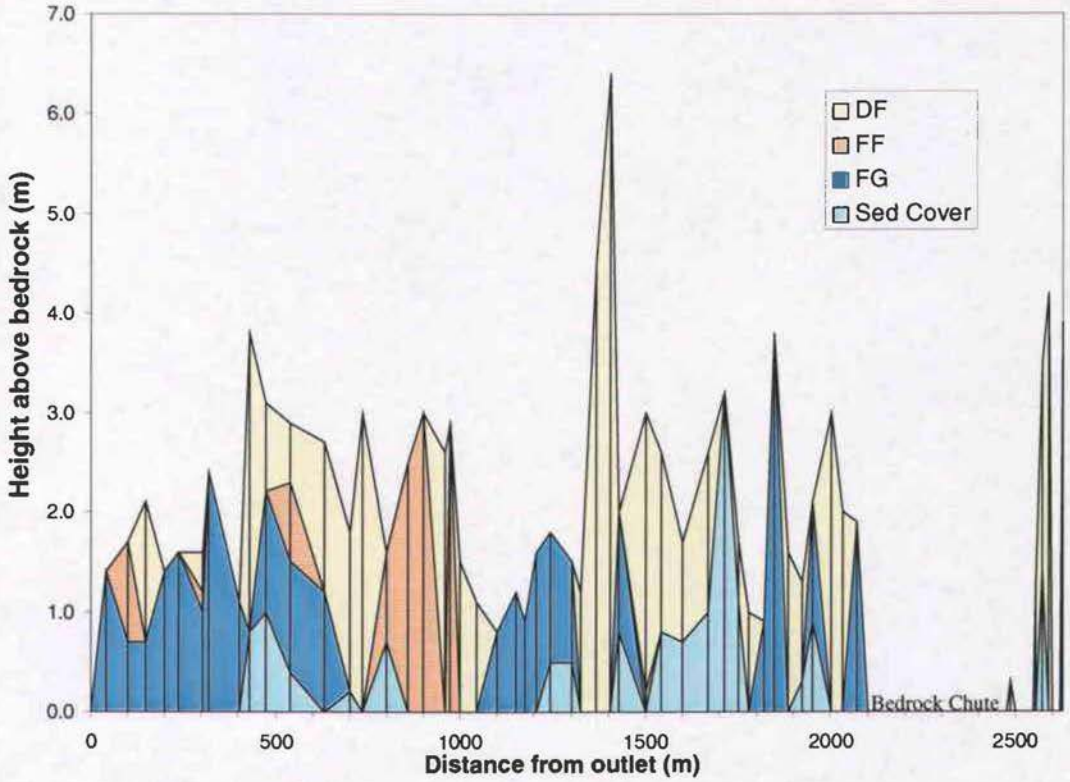

Figure 6. Channel bank stratigraphy. The vertical lines are the locations of measured stratigraphic columns. Interpolations are added for illustrative purposes and are not a detailed record of survey. Three definable units were mapped as fluvially deposited fines (FF), coarse fluvial gravels (FG), and debris flows (DF) along the main-stem channel including debris fans at tributary junctions. In locations where sediment formed distinct wedges, the estimated thickness of sediment cover (Sed Cover) is added to the height of the columns.

Sampling Locations for Radiocarbon Dating

For the purpose of sampling radiocarbon ages of sediment on the valley floor, the main-stem valley of Bear Creek was divided into two reaches: lower (0-1300 m from the outlet at Knowles Creek) and upper (1300-2600 m from the outlet). The Bear Creek watershed has an area of 2.23 km^2 (Figure 7). The watershed area at the downstream end of the upper reach is 1.32 km^2. Because of the large volume of sediment to date and its uneven distribution within the basin (Figure 5), a sampling protocol was designed to assign locations for sampling by

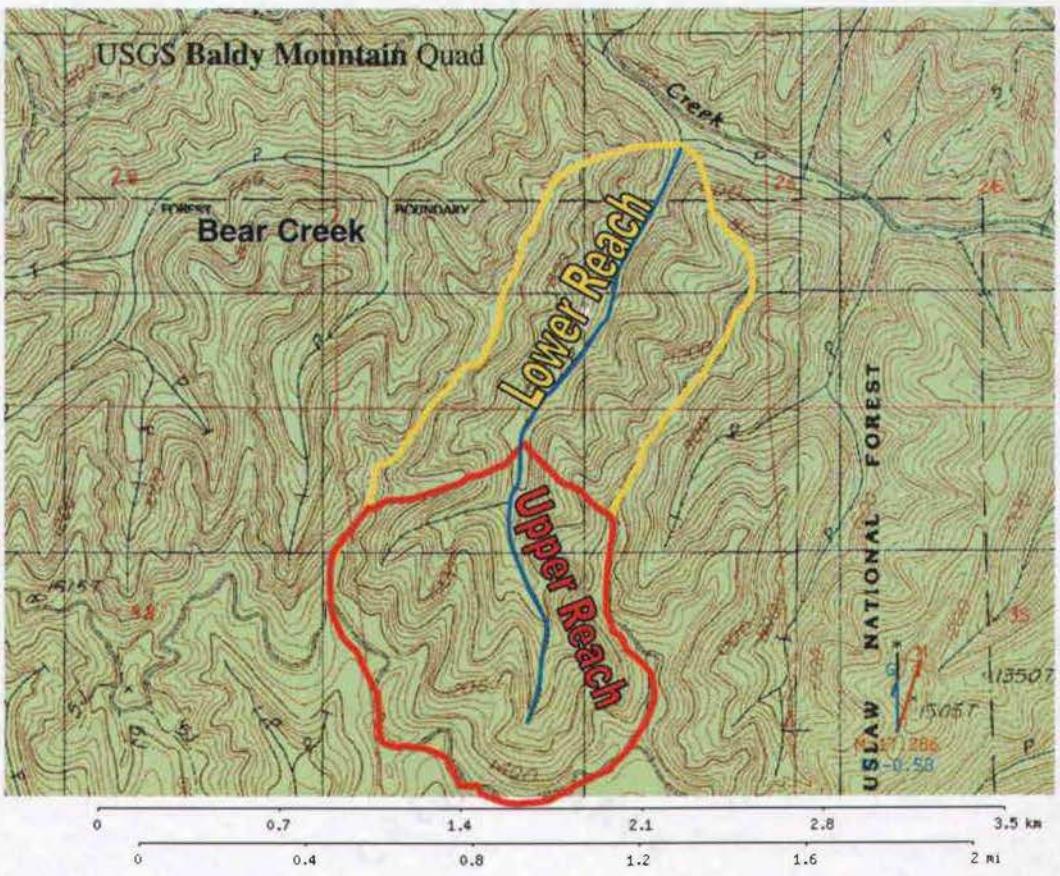

Figure 7. Bear Creek upper and lower reaches. The watershed area at the downstream end of the upper reach is 1.32 km^2. The Bear Creek watershed area is 2.23 km^2. Valley floor sediments along the main stem of Bear Creek were sampled for radiocarbon dates as separate populations in each of the upper and lower reaches.

randomly generating coordinates within the sampling space. The utility of a random sampling scheme was to reduce bias in the distribution of ages selected. For example, during a pilot study to test whether material could be found to date, two samples were collected in Bear Creek that yield radiocarbon ages of 4340±70 years before present (yr BP) and 3470±40 yr BP at two different locations. Not only did this pilot study indicate that there was significantly old material in the valley fill but also that it was likely to be over-sampled relative to younger material. These sampling locations each had interesting stratigraphic associations and/or "looked" old. A random sampling scheme forced sampling of younger and/or less interesting deposits that account for most of the distribution of ages according to sediment volume. Also, the number of definable stratigraphic units and distributions of ages within those units would make determining age distributions based on detailed stratigraphic mapping prohibitively expensive because of the number of samples to date. Also, to scale age distributions such that they represented the volume to be dated, volume estimates of each unit dated would have to be accurately known. Since not all of the sediment could be dated, random sampling provided a tool for making choices about how many samples to collect, where to collect them and, importantly, where to leave them alone. Not only did random sampling force dating of less interesting deposits but it forced skipping over some very interesting deposits. Thus, the random sampling protocol described below, allowed for the least-biased determination of age distributions for the sediment volume in each of the upper and lower reaches.

Sampling locations within each reach for radiocarbon dating were chosen by generating random coordinates according to a uniform distribution within the surveyed volume of valley fill sediment (X,Y,Z) shown in Figure 5. Streamwise distances (X coordinates) were restricted to locations of surveyed cross-sections. To ensure that valley reaches with less sediment were not over-sampled, distances from the right-hand valley wall (Y coordinate) and heights above the sediment-

bedrock interface (Z coordinate) were generated in a rectangular space defined by the maximum width and thickness of valley fill within the entire reach. Thus many generated points were rejected because they did not fall within the surveyed cross-section. Figure 8 is a schematic diagram of surveyed cross-sections with randomly generated points.

Valley fill thickness above bedrock (Z) at a particular cross section was randomly chosen within either the right or left bank. For accepted points, right or left bank locations (with equal probability) were substituted for distance from the right valley wall (Y coordinate). This substitution assumes that the locations of the channel banks with respect to the valley walls are random, uniformly distributed, and independent of other bank locations at cross sections in the reach. The observed flat bedrock of the valley floor is consistent with the assumption that the channel's lateral position at any time is randomly and uniformly distributed within the sediment fill. Also, the mean interval between cross-sections is greater than the mean length of bends of the channel, and therefore, the assumption of independence among cross sections appears reasonable. For each of the lower and upper reaches 30 sampling coordinates were generated. These

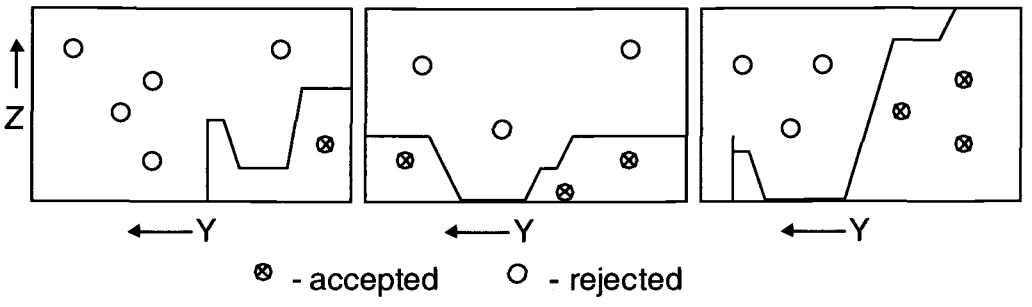

Figure 8. Schematic displaying surveyed cross-sections at different streamwise distances (X). Random coordinates are generated within a rectangular space defined by maximum width (Y) and thickness (Z) of valley fill within each sampled reach. Thus many randomly generated coordinates are rejected because they do not fall within the sediment volume.

sampling coordinates are shown on the longitudinal stratigraphic cross-section in Figure 9.

The longitudinal channel profile was surveyed with tape measure, hand level, and stadia rod. At intervals of ~10 channel widths, valley cross sections were surveyed. These cross sections were closer together, as needed to accurately measure the volume of sediment in the valley. Longitudinal distances were then measured with respect to the channel centerline. Actual sampling locations were found within ~2 m streamwise distance (X) and 0.1 m in height above bedrock (Z) of the prescribed locations. To find pieces of datable material that were representative of the sedimentary deposits, pits were excavated laterally into the channel banks by as much as 0.5 m. In places where sediment (typically gravel) covered bedrock, height above bedrock (Z) was estimated by adding height above the riverbed plus the estimate of sediment wedge thickness at that location. In a few rare instances, the sampling locations fell below the thickness of the in-stream sediment wedge. At these locations, pits were excavated into the streambed and then into the more consolidated channel bank. Due to the small sample size (>5 mg) criteria of accelerator mass spectrometry measurements of radiocarbon, and careful excavation of deposits, datable material was found in every sampling location.

The substitution of channel bank for random lateral coordinate (Y) makes use of the excavation done by the stream channel to expose the full thickness of valley fill at a particular streamwise distance. This method requires a channel that has incised into most of the thickness of the valley fill to expose bedrock at the base. This is not always the case however. For example, the channel has not had sufficient time to incise a recent (winter, 1996 AD) valley-filling debris-flow deposit in the upper reach. Random coordinates that fell within this volume were assigned the known age of this particular deposit.

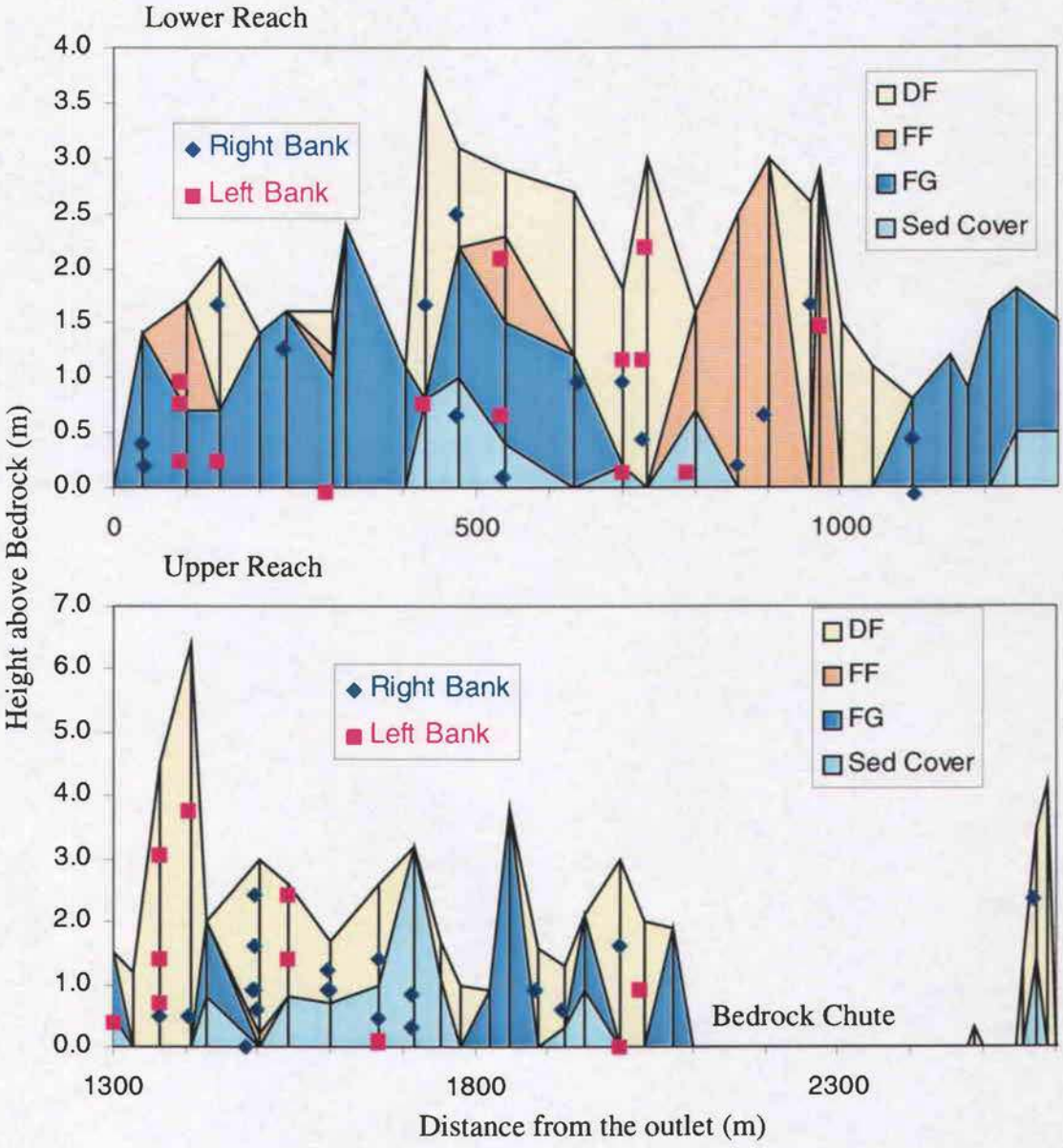

Figure 9. Randomly generated sampling coordinates. Coordinates are displayed on a longitudinal stratigraphic cross-section as drawn from columns in channel bank exposures at surveyed valley cross-sections (indicated by vertical lines) along the streamwise distance from the outlet at Knowles Creek. Stratigraphic interpolations between surveyed columns are illustrative only and are not a detailed record of survey. Each reach has 30 randomly generated points. DF = Debris flow deposit, FF = Fluvially deposited fines, FG = Coarse fluvial gravels, Sed Cover = indicates where the channel bedrock is covered with sediment.

Because sampling locations were chosen at discrete, surveyed cross-sections, a given bank profile often contained more than one sampling location. In order to reduce costs, samples lower in section were dated first to see if they were young (< 300 years before present). If young, then upper samples were assigned the age of the lower sample. Because of fluctuations in the production of C-14 in the atmosphere, calendar calibrations of recent dates will yield a wide range in the time period of 1650 AD to 1950 AD. Young dates could also be post-bomb (after 1950 AD). This use of superposition minimizes repeated samples of large, overlapping date ranges.

Erosion Rates from Valley Residence Times

Assuming that the valley fill within the basin is in an approximate flux steady state over the timescale of the mean residence time of the deposits, i.e. its volume remains relatively constant and sediment is added and removed in equal proportion over time, the basin-average erosion rate is

$$E = \frac{\rho_d V}{\rho (\mu_T A)} \qquad (1)$$

where E is erosion rate (m/yr); ρ_d is the average deposit dry bulk density; ρ is the parent rock bulk density; V is the volume of the valley fill (m^3); μ_T is the mean residence time of the valley fill (yr); and A is contributing area (m^2).

The mean of the randomly sampled radiocarbon ages represents the mean age used above to calculate erosion rates in equation (1). Radiocarbon ages truly only represent storage to present and not the residence times but serve as a proxy for residence times. Assuming that sediment erosion and transport are in a flux steady state over the time interval of radiocarbon ages, the storage age distribution will approximate the residence time distribution. Mean age (μ_T) can also be

determined independently of the radiocarbon ages, if an independent measure of the erosion rate (E) of the basin is used to solve equation (1).

Residence Time Distributions

The residence time distribution for sediment stored on the valley floor represents a transfer function between inputs and outputs and depends on the interactions between deposition and transport processes. The valley floor reaches dated above can be considered as reservoirs that receive pulse inputs of sediment from debris flows and more gradual outputs by fluvial processes. If the residence times follow an exponential distribution, then the reservoir of sediment represented by the valley floor deposits is "fully mixed" i.e. all sediments in the valley have equal probability of removal at a given time. A pulse of sediment from a given time is represented in the valley's sediment output in proportion to its relative volume in storage. Mixing in this sense is not due to the actual sediments moving around in the reservoir so much as that the channel's position changes over time in the reservoir and more importantly that the channel cuts through deposits representing a wide range of ages. Thus, a wide age-range of sediment is likely to be removed at a given time. Both actual sediment mixing due to fluvial reworking and that resulting from channel position in the sediment are expected to result from a combination of lateral erosion in response to excess sediment load and channel avulsion due to damming by woody debris and debris flows. At the extreme alternative to a fully mixed system with an exponential residence time distribution is a system characterized by "plug flow" i.e., the last sediment to enter is usually the last sediment to leave. Thus, in this case, it is expected that the residence time distribution would be strongly peaked at a non-zero age and have a narrow range in ages (e.g. Harleman, 1990).

The residence time distribution was determined by summing the probability distributions of the radiocarbon ages. To distinguish among the two

extremes of the residence time distribution, a dispersion number is calculated from the distribution. The dispersion number (d) is

$$d = \frac{D}{uL} \tag{2}$$

where D is the longitudinal dispersion coefficient (m^2/yr), u is the mean velocity of sediment through the reservoir (m/yr), L is the length of the reservoir (m), and d is the dispersion number (dimensionless). For a fully mixed reservoir, $d \rightarrow \infty$; for plug flow, $d = 0$. The mean and the variance of the distribution are related to the dispersion number by

$$\frac{\sigma_T^2}{\mu_T^2} = 2d - 2d^2\left(1 - e^{-\frac{1}{d}}\right) \tag{3}$$

where σ^2_T is the residence time variance, μ_T is the mean residence time. Equation (3) was solved implicitly for the dispersion number, and given the mean velocity of sediment, u, equation (2) was solved for the longitudinal dispersion coefficient. The mean velocity of sediment is

$$u = \frac{L}{\mu_T} \tag{4}$$

Levenspiel and Bischoff (1968) found that the number, n, of reservoirs in a series was approximately related to the dispersion number of an equally dispersive reservoir, and this relationship may be approximated as (Harleman, 1990)

$$n \approx \left(\frac{1}{2d} + \frac{1}{2}\right) \tag{5}$$

The residence time distribution for n reservoirs in a series is

$$f_t(t) = \frac{n^n}{(n-1)!}\left(\frac{t}{\mu_T}\right)^{n-1} e^{-\frac{nt}{\mu_T}}. \qquad (6)$$

which is a special case of the Erlang distribution (Drake, 1967). For $n = 1$, the Erlang distribution is equal to an exponential distribution.

For a sample distribution and its calculated mean and variance and, thus, dispersion number, a theoretical distribution is hypothesized from (5) and (6) and tested for a goodness of fit against the sample distribution with a two-stage δ-corrected Kolmogorov-Smirnov test (KST) (Khamis, 2000; Benjamin and Cornell, 1970).

RESULTS AND ANALYSIS

Radiocarbon Ages

Of 60 random sampling locations, 54 carbon samples were collected. Radiocarbon ages were determined by accelerator mass spectrometry for 33 samples and beta decay counting for 11 samples. The remaining 10 carbon samples were assigned ages on the basis of superposition (Table 1, Figures 10 and 11). The remaining 6 random sampling locations not collected fell within a valley filling debris flow deposit that occurred in the calendar year 1996 AD and were assigned an age of zero for purposes of further analysis. For the purposes of plotting and analysis, all 60 sampling points are included with each age carrying equal weight whether analytically determined or stratigraphically assigned.

Figure 12 shows probability density plots of calendar calibrated dates for each of the upper and lower reaches that were constructed using the program OxCal Version 3.9 (Ramsey, 2003). Due to complexity in the calibration curve, multiple calendar-calibrated dates can be returned for a single radiocarbon age. To simplify analysis and avoid artifacts of the calibration curve, radiocarbon ages were used for calculating dispersion coefficients and goodness of fit testing.

Erosion Rates

Erosion rates were calculated using equation 1 (Table 2). To calculate the erosion rate for the entire basin a weighted-average of the mean ages for the upper and lower reaches was calculated using the volumes. To account for the density change between rock and sediment, values of 2.27×10^3 kg m^{-3} for weathered bedrock and 7.40×10^2 kg m^{-3} for soil were used to scale the lower limit on the erosion rate (Anderson et al., 2002). The upper limit is has no density adjustment.

Table 1. Radiocarbon samples, locations, characteristics, and ages

Valley Reach	Station	Dist. (m)	Bank	Height (m)	Strat.	Mat.	Meth.	Mass (g)	Lab Number	Radiocarbon Age±1sigma
Lower	BC-1	44	R	0.45	FG	dw	INF	0.33		60 ± 50
	BC-2	147	R	1.7	DF	dc	AMS	0.23	AA57073	410 ± 34
	BC-3	147	L	0.3	FG	dc	AMS	0.29	AA57074	1970 ± 36
	BC-4	94	L	0.8	FF	dc	AMS	1.13	AA57075	179 ± 30
	BC-5	236	R	1.3	DF	dc	AMS	0.12	AA57076	1706 ± 27
	BC-6	294	L	0.01	FG	sl br	BD	60.48	B184181	130 ± 50
	BC-7	430	R	1.7	DF	dc	AMS	0.27	AA57077	1056 ± 29
	BC-8	429	L	0.8	FG	dc	AMS	0.45	AA57078	205 ± 30
	BC-9	473	R	1.5+1	DF	dc	AMS	0.15	AA57079	1044 ± 32
	BC-10	473	R	0.7	FG	dc	AMS	0.01	AA57080	2334 ± 33
	BC-11	533	L	0.3+0.4	FF	dc	AMS	0.26	AA57081	3401 ± 33
	BC-12	533	L	1.7+.0.4	FF	dc	AMS	0.26	AA57082	2913 ± 32
	BC-13	640	R	1	DF	dw	AMS	2	AA57083	437 ± 29
	BC-14	700	R	0.8+0.2	DF	w	BD	29.89	B184182	450 ± 50
	BC-15	700	L	1+0.2	FF	wb	BD	26.95	B184183	110 ± 50
	BC-16	700	L	0+0.2	FG	sl br	BD	38.5	B184184	130 ± 50
	BC-17	727	L	1.2	DF	dc	AMS	0.33	AA57084	1474 ± 29
	BC-18	731	L	2.2	DF	dc	AMS	0.14	AA57085	1877 ± 31
	BC-19	727	R	0.5	DF	dc	AMS	0.12	AA57086	816 ± 30
	BC-20	789	L	0.2	FF	dc	AMS	0.8	AA57087	3769 ± 30
	BC-21	858	R	0.25	FF	sl br	BD	20.91	B184185	370 ± 50
	BC-22	894	R	0.7	FF	dc	AMS	0.34	AA57088	201 ± 44
	BC-23	1101	R	0	FG	wb	BD	54.14	B184186	180 ± 50
	BC-24	971	L	1.5	FF	dc	AMS	0.39	AA57089	2491 ± 25
	BC-25	959	R	1.7	DF	dc	AMS	0.04	AA57090	2670 ± 27
	BC-26	94	L	0.3	FG	dc	AMS	0.02	AA57091	4447 ± 40
	BC-27	46	R	0.25	FG	w	BD	147.61	B184187	60 ± 50
	BC-28	1100	R	0.5	FG	br	INF	3.08		180 ± 50
	BC-29	94	L	1	FF	dw	INF	2.9		179 ± 30
	BC-30	538	R	0.15	FG	dc	AMS	0.15	AA57092	1267 ± 31
Upper	BC-31	1298	L	0.5	FG	dw	AMS	3.51	AA57093	Post-bomb
	BC-32	1365	L	0.8	DF	dc	AMS	0.17	AA57094	402 ± 31
	BC-33	1365	L	1.5	DF	dc	AMS	0.08	AA57095	1532 ± 31
	BC-34	1365	L	3.1	DF	dc	AMS	0.45	AA57096	1128 ± 31
	BC-35	1365	R	0.6	DF	dw	AMS	0.25	AA57097	623 ± 34
	BC-36	1405	R	0.6	DF	dc	AMS	0.02	AA57098	2443 ± 33
	BC-37	1405	L	3.8	DF	dc	AMS	0.05	AA57099	655 ± 30
	BC-38	1496	R	1	DF	dc	AMS	0.04	AA57100	213 ± 30
	BC-39	1496	R	1.7	DF	dc	INF	0.03		213 ± 30
	BC-40	1499	R	0.7	DF	dc	INF	0.04		213 ± 30
	BC-41	1485	R	0.1	DF	dc	INF	0.04		213 ± 30
	BC-42	1492	R	1	DF	dc	INF	0.02		213 ± 30

Valley Reach	Station	Dist. (m)	Bank	Height (m)	Strat.	Mat.	Meth.	Mass (g)	Lab Number	Radiocarbon Age±1sigma
Upper (cont.)	BC-43	1496	R	2.5	DF	dc	AMS	0.02	AA57101	3741 ± 35
	BC-44	1541	L	1.5	DF	dc	AMS	0.01	AA57102	167 ± 30
	BC-45	1541	L	2.5	DF	sl br	INF	7.45		167 ± 30
	BC-46	1597	R	1	DF	dw	AMS	2.37	AA57103	126 ± 30
	BC-47	1597	R	1.3	DF	w	INF	9.24		126 ± 30
	BC-48	1600	R	1	DF	dc	INF	0.06		126 ± 30
	BC-49	1884	R	1	DF	w	AMS	5.15	AA57104	Post-bomb
	BC-50	1922	R	0.7	DF	br	BD	50.68	B184188	Post-bomb
	BC-51	2000	R	1.7	DF	sl br	AMS	6.85	AA57105	437 ± 41
	BC-52	2000	L	0.1	DF	br	BD	15.35	B184189	Post-bomb
	BC-53	2029	L	1	DF	wb	BD	11.75	B184190	40 ± 60
	BC-54	2572	R	2.4	DF	sl br	BD	133.64	B184191	510 ± 50
Deposit ages locations not collected										
	55	1667	R	0.55	DF		INF			0
	56	1667	R	1.5	DF		INF			0
	57	1667	L	0.16	DF		INF			0
	58	1667	L	0.21	DF		INF			0
	59	1714	R	0.41	DF		INF			0
	60	1714	R	0.93	DF		INF			0

Table 1. Radiocarbon ages collected and inferred ages for sampling points (shaded). Dist. = Distance from outlet. Height = Height above sediment-bedrock interface, R = Right bank, L = Left bank, DF = Debris flow deposit, FF = Fluvially deposited fines, FG = Coarse fluvial gravel, dw = detrital wood, dc = detrital charcoal, w = wood, sl br = streamlined wood branch, br = branch, AMS = age determination by accelerator mass spectrometry, BD = beta decay counting, INF = age inferred on the basis of relative stratigraphic position. The NSF University of Arizona Accelerator Mass Spectrometer Facility determined AMS ages. BD ages were determined by Beta Analytic. Ages are radiocarbon years before present (1950 a.d.) with one standard deviation calculated error based on combined measurements of the sample, background and modern reference standards.

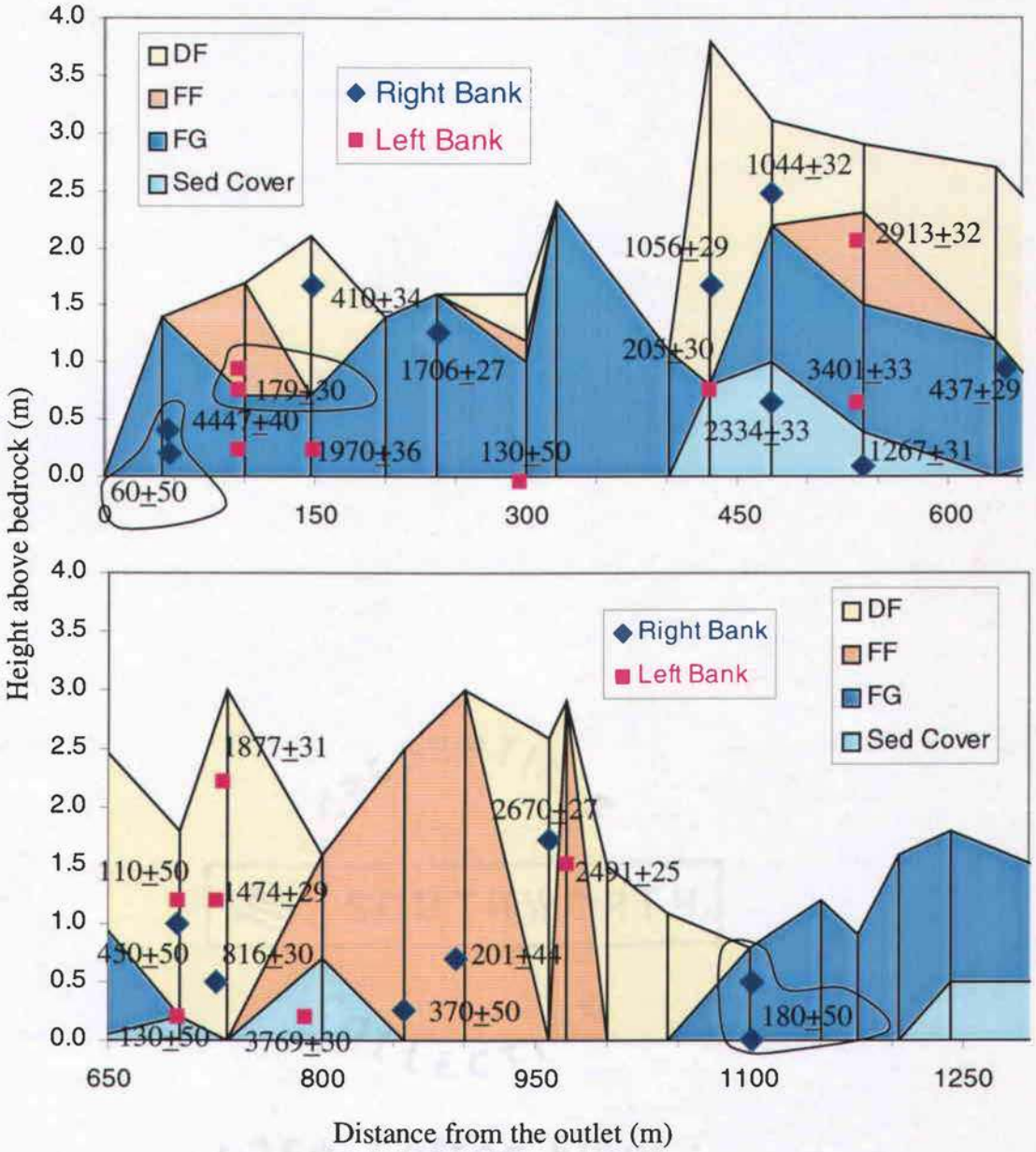

Figure 10. Radiocarbon ages mapped in the lower reach channel banks. Stratigraphy is the same as in Figures 6 and 9. Diamonds show right bank samples. Squares are left bank samples. Encircled multiple sampling points within a single left or right bank column indicate where upper column samples were assigned the age of the lower dated sample.

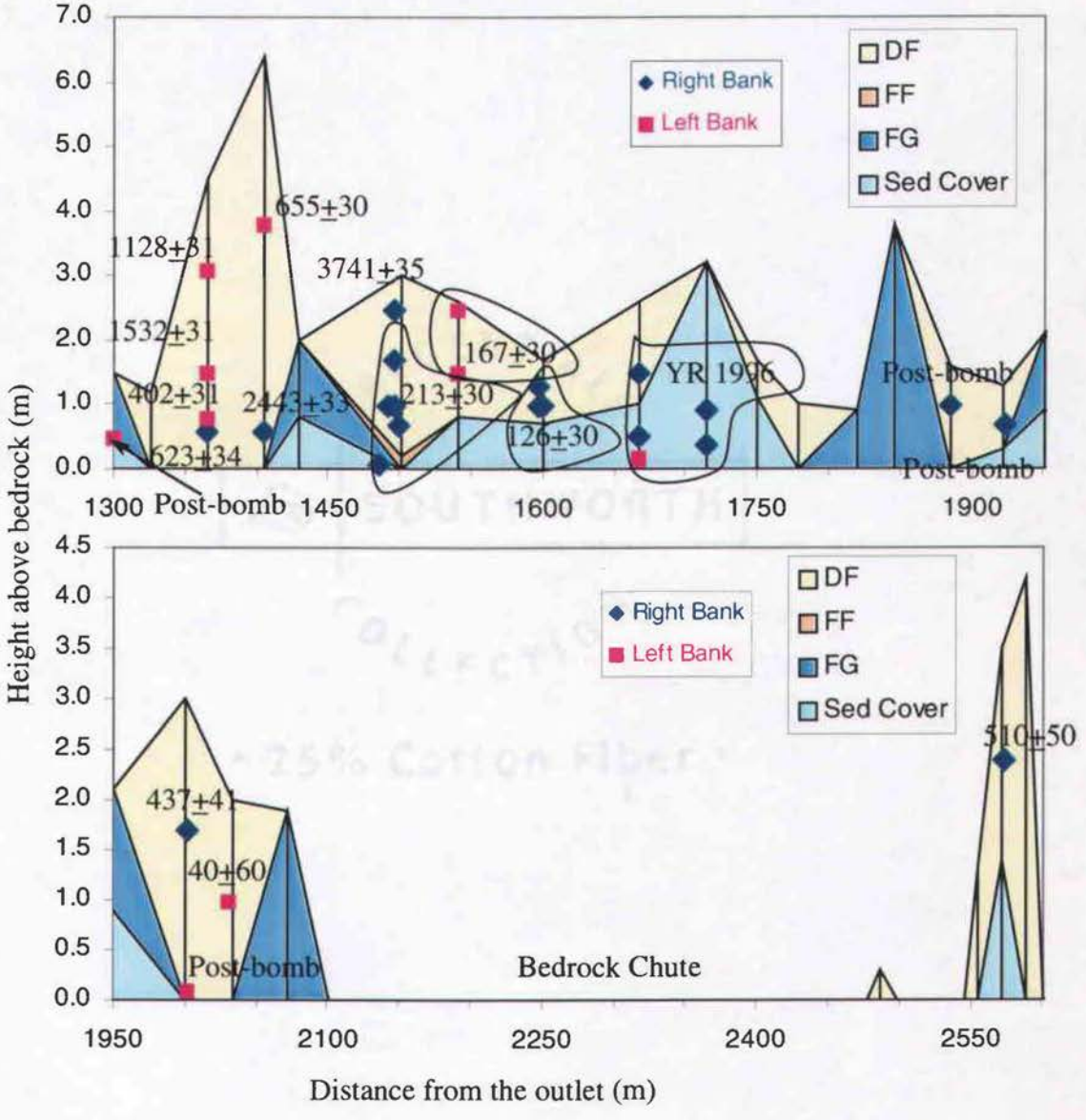

Figure 11. Radiocarbon ages mapped in the upper reach channel banks. Stratigraphy is the same as in Figures 6 and 9. Diamonds show right bank samples. Squares are left bank samples. Encircled multiple sampling points within a single left or right bank column indicate where upper column samples were assigned the age of the lower dated sample. Sampling points that fell within the 1996 debris flow deposit are also indicated. Multiple ages in the column at 1496 meters were assigned the same age based on the young date and determination of the deposit as a single event debris flow.

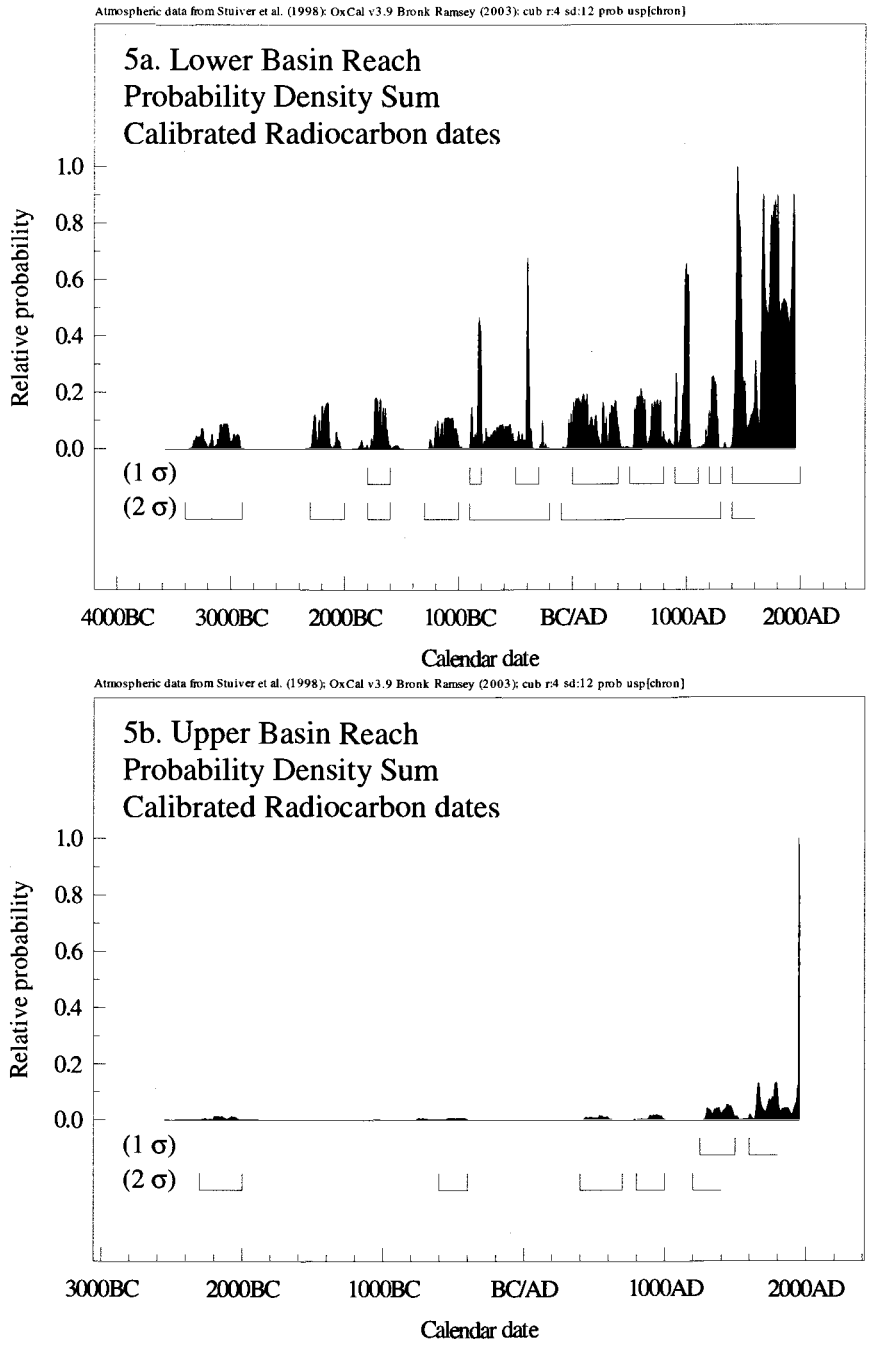

Figure 12. Valley floor sediment calendar dates. Lower reach (a.) and upper reach (b.) calendar calibrated probability density distributions of radiocarbon ages presented in Table 1 and Figures 10 and 11. Upper brackets show 68.2 % (1 σ) probability date ranges. Lower brackets show 95.4 % (2 σ) probability.

Sediment Reservoir Characteristics:	Lower Basin	Upper Basin	Full Basin
Volume (m^3)	4.72×10^4	2.23×10^4	6.95×10^4
Reservoir Length (m)	1.3×10^3	1.3×10^3	--
Mean Age (yr)	1.22×10^3	4.43×10^2	9.96×10^2
Mean velocity through reservoir (m/yr)	1.1	2.9	--
Contributing Area (km^2)	--	1.32	2.23
Basin Inferred **Erosion Rate** (mm/yr)	--	0.013 – 0.038	0.011 – 0.033

Table 2. Sediment characteristics and erosion rates. The mean velocity through each reservoir was calculated by dividing the reservoir length by the mean age. Erosion rates were calculated using equation 1. A volume weighted average age of the upper basin and lower basin ages provides the mean age for the full basin. The lower limit on the erosion rate includes a density adjustment due to the conversion of weathered bedrock to soil. The upper limit on the erosion rate includes no density adjustment.

Residence Time Distribution: The Dispersion Number

For each of the lower and upper basin sediment reservoirs, dispersion numbers (d) were calculated of approximately 2×10^7 and 2×10^8 respectively. Mean velocities (u) of 1.1 and 2.9 m/yr were calculated by dividing the length by the mean age for each reach (Table 2). Using equation 2 plus the mean velocities of sediment through each reservoir (u) and reservoir lengths (L) of 1.3×10^3 m, the longitudinal dispersion coefficients (D) are 3×10^{10} and 8×10^{11} m^2/yr for each of the lower and upper reach sediment reservoirs, respectively. The high dispersion numbers imply that the reservoirs are approaching fully mixed. Using equation (5), these dispersion numbers imply a series of n = ½ reservoirs. Since the Erlang distribution (6) only accepts positive integer values of n, it can be inferred that the value of n has to be at least 1. Importantly, the calculation has shown that the dispersion number is not small, and thus n is not 2 or greater which would imply some aspect of plug flow. Thus each reservoir is approaching fully mixed conditions.

Goodness of Fit Test

The goodness of fit of the hypothetical distribution with the empirical data was tested using a two-stage δ-corrected Kolmogorov-Smirnov test (KST) (Khamis, 2000, Benjamin and Cornell, 1970). This test does not directly compare the probability density function (PDF) but rather the associated cumulative distribution functions (CDF). The classical KST compares the largest of the absolute values of the *n* differences between the empirical CDF and the hypothesized CDF with a statistic based on the sample size and desired level of significance (Benjamin and Cornell, 1970). The δ-corrected KST improves the statistical power by modifying the definition of the empirical CDF and employing two tests (Khamis, 2000). The radiocarbon ages were used to construct a summation of probability density distributions (Figure 13) analogous to the calendar calibrated distributions in Figure 12 (eg. Meyer et al. 1995, Wegmann and Pazzaglia, 2002). These probability density distributions were then used to calculate the smoothed cumulative distributions for the radiocarbon dates in each reach (Figure 14). The discrete cumulative distributions were used to test the hypothesis that the valley floor acts as a fully mixed reservoir. The mean age of each reach parameterized a cumulative exponential distribution function of the form:

$$P(t)= 1-e^{(-t/\mu_T)} \qquad (7)$$

where P is the probability cumulative distribution function (CDF), t is the age of the sample before present and μ_T is the mean age of the distribution. An exponential distribution of residence times suggests that the valley floor reservoir of sediment is fully mixed (e.g. Harleman, 1990).

The calculations for the two-stage δ-corrected KST are shown in Table 3. The null hypothesis states that the observed cumulative histogram follows an exponential distribution with the same mean age as that of the observed data. The

alternate hypothesis simply states the observed cumulative histogram does not follow an exponential distribution with the same mean age as that of the observed data. For the lower reach, the test fails to reject the null hypothesis at the 5% significance level, a result that is consistent with the hypothesized well-mixed reservoir that acts as a capacitor to episodic sediment input. For the upper reach the test rejects the null hypothesis in favor of the alternate hypothesis at the 5% significance level. In this upper reach, then, the statistical test does not support the hypothesis that the valley floor behaves as a well-mixed reservoir.

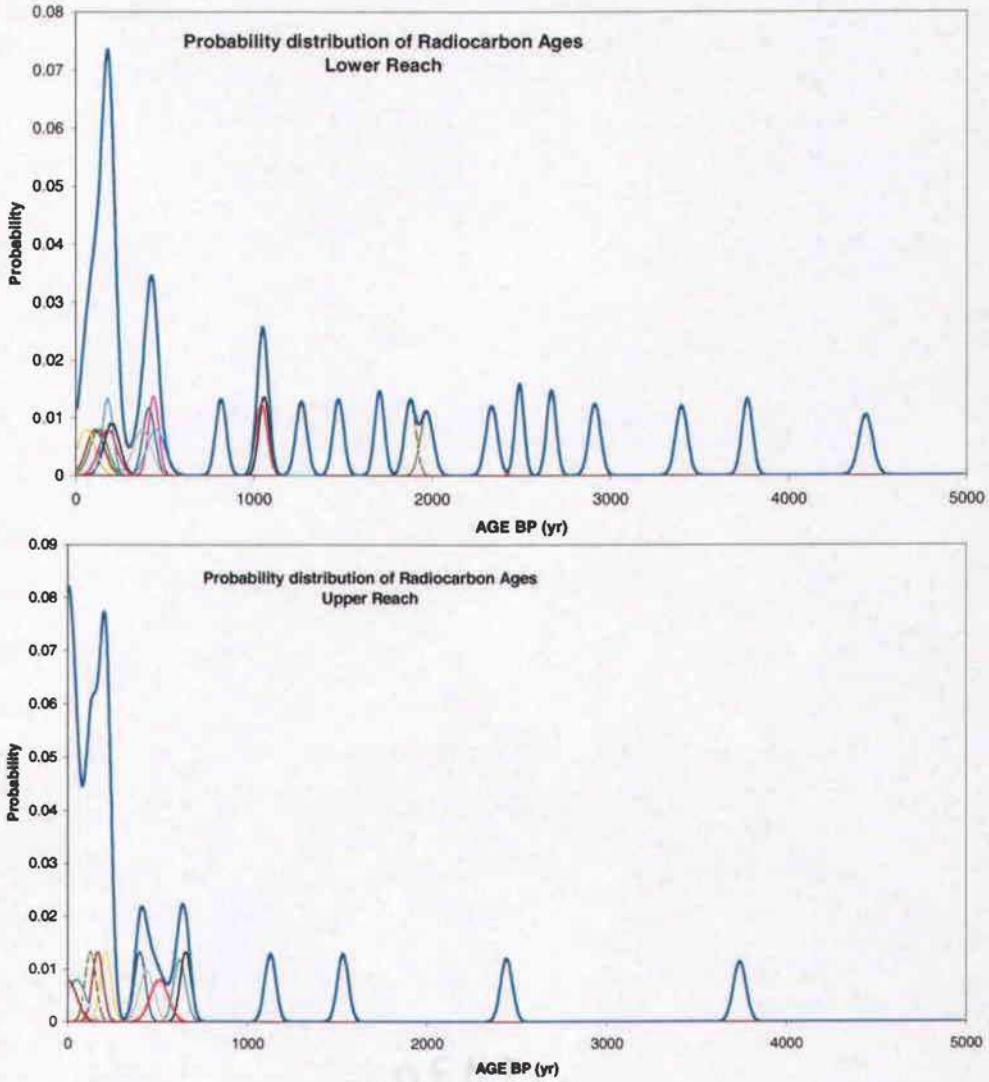

Figure 13. Probability distributions for radiocarbon ages. Each age defines the peak of a normal distribution with a laboratory-reported standard deviation defining the rest of the distribution. Gauss curves are then summed to define the probability density distribution function for each reach. This figure is analogous to Figure 12 except that radiocarbon ages instead of calendar calibrated dates are used to construct the distributions.

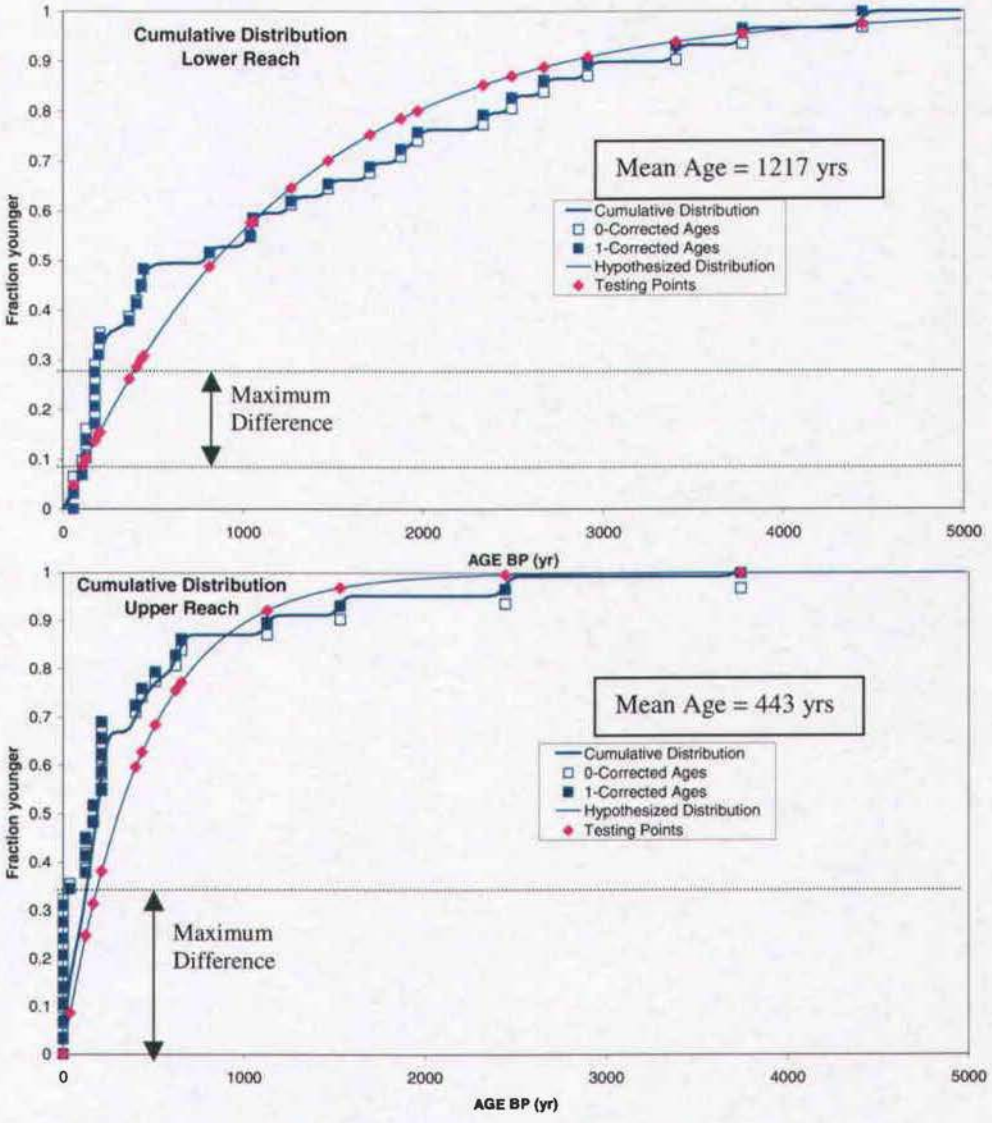

Figure 14. Cumulative age distribution functions for each of the upper and lower basin reaches. Hypothesized distributions are calculated using equation 7. The mean ages define the fractions that are younger than $1\text{-}e^{-1}$ or ~0.63. The testing points (diamonds) are where the measured ages intersect the hypothesized distribution and are the points at which the two-stage δ-corrected Kolmogorov-Smirnov test are performed. The solid cumulative distribution lines represent the integrals of the distributions in Figure 13. The individual age points are plotted by ranking the ages in order from $i = 1$ to $i = 30$ for each reach and assigning each age a value in the cumulative distribution of i divided by 31 for the 0-corrected test (open squares) and i minus one then divided by 29 for the 1-corrected test (closed squares).

Table 3. Calculations for Two-Stage δ-Corrected Kolmogorov-Smirnov Test							
Lower Reach				Upper Reach			
i	Age t_i	0-corrected $\lvert i/(n+1)-P(t_i)\rvert$	1-corrected $\lvert(i-1)/(n-1)-P(t_i)\rvert$	i	Age t_i	0-corrected $\lvert i/(n+1)-P(t_i)\rvert$	1-corrected $\lvert(i-1)/(n-1)-P(t_i)\rvert$
1	60	0.0159	0.0481	1	0	0.0323	0.0000
2	60	0.0164	0.0136	2	0	0.0645	0.0345
3	110	0.0103	0.0175	3	0	0.0968	0.0690
4	130	0.0277	0.0021	4	0	0.1290	0.1034
5	130	0.0600	0.0366	5	0	0.1613	0.1379
6	179	0.0567	0.0356	6	0	0.1935	0.1724
7	179	0.0890	0.0701	7	0	0.2258	0.2069
8	180	0.1206	0.1039	8	0	0.2581	0.2414
9	180	0.1528	0.1384	9	0	0.2903	0.2759
10	201	0.1703	0.1581	**10**	**0**	**0.3226**	**0.3103**
11	**205**	**0.1998**	**0.1898**	11	40	0.2685	0.2585
12	370	0.1249	0.1171	12	126	0.1395	0.1317
13	410	0.1333	0.1277	13	126	0.1718	0.1662
14	437	0.1499	0.1465	14	126	0.2040	0.2007
15	450	0.1747	0.1736	15	167	0.1698	0.1687
16	816	0.0275	0.0286	16	167	0.2020	0.2031
17	1044	0.0276	0.0243	17	213	0.1666	0.1700
18	1056	0.0005	0.0061	18	213	0.1989	0.2044
19	1267	0.0341	0.0263	19	213	0.2311	0.2389
20	1474	0.0571	0.0470	20	213	0.2634	0.2734
21	1706	0.0765	0.0643	21	213	0.2957	0.3079
22	1877	0.0765	0.0620	22	402	0.1132	0.1276
23	1970	0.0600	0.0433	23	437	0.1148	0.1315
24	2334	0.0789	0.0600	24	510	0.0904	0.1093
25	2491	0.0645	0.0433	25	623	0.0514	0.0726
26	2670	0.0499	0.0265	26	655	0.0666	0.0900
27	2913	0.0378	0.0122	27	1,128	0.0507	0.0251
28	3401	0.0357	0.0079	28	1,532	0.0653	0.0375
29	3769	0.0194	0.0107	29	2,443	0.0605	0.0305
30	4434	0.0061	0.0261	30	3,741	0.0320	0.0002
N	δ	α = 0.05	Max	N	δ	α = 0.05	Max
30	0	0.222	0.1998	30	0	0.222	0.3226
30	1	0.232	0.1898	30	1	0.232	0.3103

Table 3. Calculations for the two-stage δ-corrected KST. This test compares the largest of the absolute differences between the hypothesized (equation 7) and empirical cumulative distributions shown in figure 14. The lower reach test fails to reject the null hypothesis that the two distributions are the same. The upper reach test rejects the null hypothesis in favor of the alternative hypothesis.

DISCUSSION

Erosion Rates

Erosion rates calculated using radiocarbon dating for the two contributing areas are in good agreement with one another (Table 3) and indicate that the basin is in a flux steady state over the time-scale of sampled radiocarbon ages. These rates are minimum rates because of the possible inherited age in radiocarbon samples and reworking of previously deposited material. Inherited age is the time that a piece of wood or charcoal spends between the death of the tree and its incorporation into the sedimentary deposit, thus increasing the measured age of the deposit. To test for inherited age a piece of wood identified as a weathered-out knot from a tree was pulled from a recently carved channel in a debris flow deposit estimated to be about 20 years old from tree-rings of an alder growing on it. This sample, BC-54 (Table 1) gave a radiocarbon age of 510$\pm$50 years BP and suggests an inherited age of 500 to 600 years when calibrated. This measure of inherited age agrees well with that determined by Gavin (2001) for charcoal in surface soil on the west coast of Vancouver Island (Canada). On Vancouver Island, 26 radiocarbon dates of charcoal were found to be 0 to 670 years older than associated forest fire ages determined by tree-ring counts. This scale of inherited age is not surprising for Pacific Northwest forests where slow tree growth rates and decay rates can add much time to a wood sample before burial in a sedimentary deposit. This inherited age may significantly reduce the actual age of the deposits and increase the erosion rates determined from them. For example, an inherited mean age of 600 years increases the full-basin erosion rate from 0.033 mm/yr to 0.086 mm/yr. The scale of this inherited age effect, though, is likely to be smaller, especially for deposits younger than 500 to 600 years that comprise the bulk of the data because the maximum possible inherited age of a given sample is the measured radiocarbon age of that sample. Indeed, because the age distributions are skewed towards younger ages, this effect should be minimal

and may likely be something like a 250 to 300 yr shift as predicted by Gavin (2001). The inherited ages will not have an impact on the general shape of the distribution but only shift some of the older dates down in age.

A second important effect in determining the age of a deposit is reworking of older deposits and associated wood or charcoal. For example, a piece of charcoal at 1496 meters upstream returned an age of 3741 yrs BP (BC-43, table 1). This charcoal piece was higher in section than BC-38 in the same column that returned an age of 213 yr BP. This suggests that this debris flow entrained older sedimentary deposits from upstream and mixed them. Indeed, this particular deposit was unusual since it was dominated by rounded fluvial gravels and boulders with few fines. It was interpreted as a debris flow due to the absence of fluvial sedimentary structures, such as imbrication and stratification, its thickness, and its matrix-supported clasts. Most other debris flows are marked by poorly sorted angular clasts within a weathered soil matrix. Although this anomalous date sheds doubt on the commonly made assumption that radiocarbon ages can be safely used to date individual events in sedimentary deposits, it does not defeat the goal of determining a residence time distribution for this valley reach. Indeed, the reworked fluvial material in this particular debris flow suggests that the deposit was previously on the valley floor, albeit upstream of its present location and is likely to have inherited ages. Hence it is likely that this radiocarbon age does provide a reliable indicator of residence time for some sediment within this reach. Also important to note is that this single age accounts for only 3 percent of the age distribution for the upper reach.

Despite the uncertainties in the reliability of the radiocarbon ages for determining the actual ages of the deposits, bank profiles with multiple sampled ages provide a method check on the use of randomly sampled radiocarbon ages. Figures 10 and 11 display the relative positions of the sampled ages within the bank profiles surveyed. In all but a few cases, radiocarbon ages obey the law of

superposition within a given bank profile. That is, older ages are lower in section than younger ages. Exceptions include that at 1496 meters described above, and age reversals at 727 meters and 1365 meters from the outlet. The reversed ages at 727 meters are actually 4 meters apart in horizontal distance (727 m and 731 m) within the left bank and thus cannot be positively confirmed as reworking or inherited age. These radiocarbon ages are 1447±29 and 1877±31 yr BP. However, assuming that the debris-flow deposit that these two ages fall within represents a single event, it can be inferred that the upper age has an inherited age of at least 430 years. With regard to the age reversal in the left bank at 1365 m, the younger age likely represents inset fill against an older bank. It was noted in the field that the upper sampling points were collected from more consolidated debris flow deposits while the lower sampling point was collected from a loose debris flow deposit. These samples were not in a vertical line but were collected from a relatively tall and sloping bank. A schematic of this age association in cross-section is shown in Figure 15.

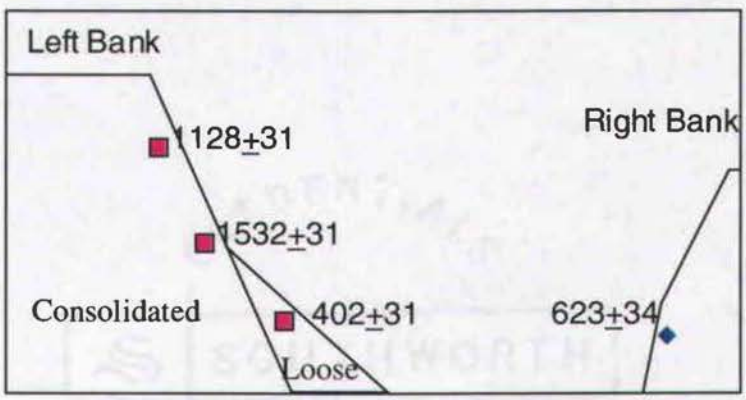

Figure 15. Schematic cross-section of bank profiles and collected radiocarbon ages at 1365 meters from the outlet. All bank units were identified as debris flow deposits. Relative positions are not to scale; scale associations are shown in Figure 11.

Given that most of the ages follow the law of superposition with explanations for the exceptions, it appears the sampled radiocarbon ages can be relied on to describe an age distribution for the sediments thus dated. Importantly, the positions of these ages argue against a possible objection that the exponential distributions may simply be a function of the preservation potential of wood and charcoal and that the deposits are all actually very close in age. Also against this suggestion is that a radiocarbon sample was selected at every random sampling point (with the exception of the 1996 debris flow deposit), i.e. wood and charcoal were not selected in proportion to their abundance. Carbon rich and poor deposits both yielded equally datable materials.

Assuming that the shape of the radiocarbon age distribution does approximate the true shape of the residence time distribution, it is possible to re-scale the distributions (shown in Figure 13) given an independent measure of the mean age of the deposits. Inherited age and reworking skew the distribution to older ages and thus imply lower erosion rates. Other studies in the Oregon Coast Range have implied erosion rates of about 0.1 mm/yr (Reneau and Dietrich, 1991, Heimsath et al., 2001). Assuming a ~0.1 mm/yr erosion rate applies to Bear Creek, it implies a mean age of 170 years for the upper reach and 361 years for the lower reach, neglecting the density correction using equation (1). Using the same density corrections used to calculate the erosion rates from the mean radiocarbon age, the mean ages further reduce to 55 years and 118 years for the upper and lower reaches, respectively. The ratios of the independently derived mean age to the radiocarbon mean age act as scaling factors to adjust the distributions shown in Figure 13. These adjusted distributions are shown in figure 16. Important to note is that this re-scaling does not change the dispersion number calculation, which is entirely based on the shape of the distribution and is dimensionless. Similarly, the re-scaling does not affect the results of the

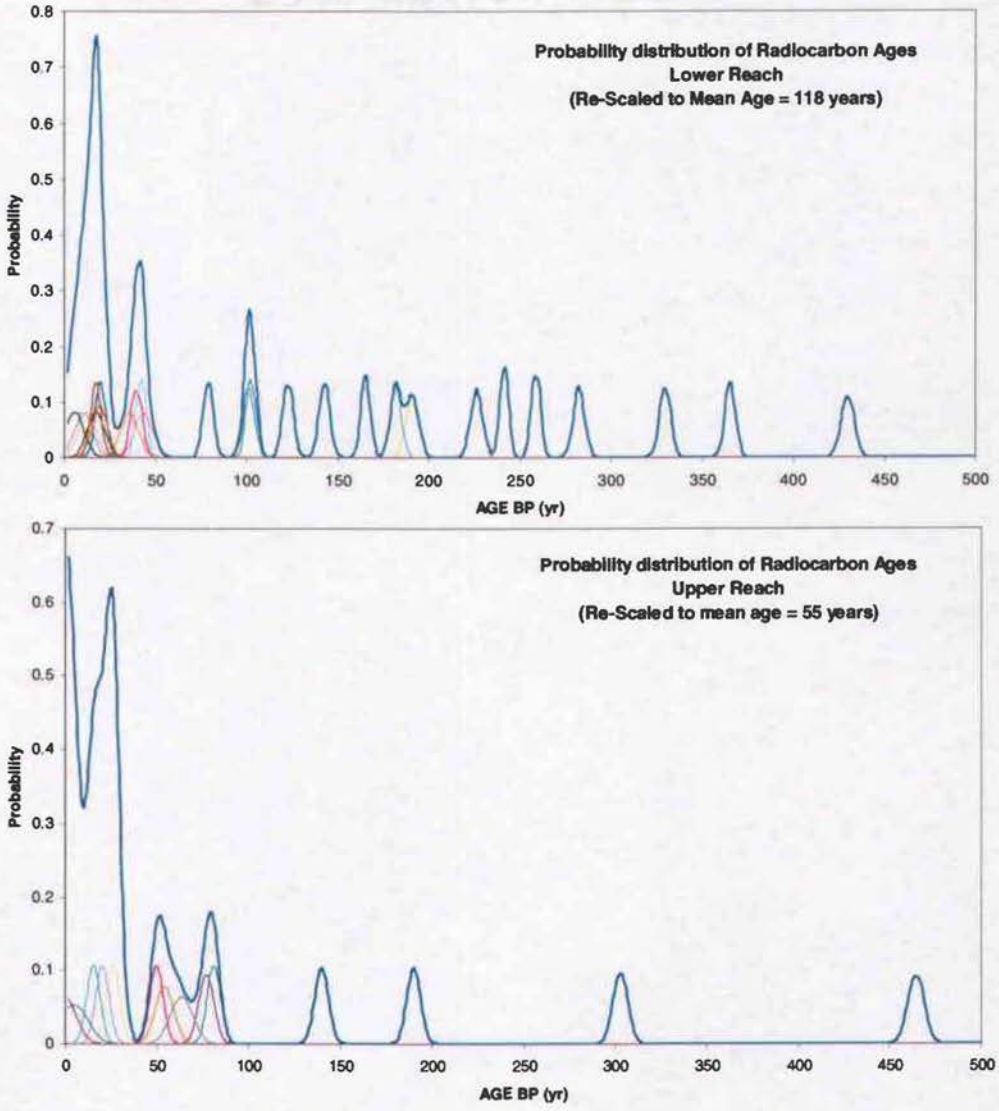

Figure 16. Probability distributions for radiocarbon ages (shown in Figure 13) re-scaled to an independently derived mean age for each of the upper and lower reaches.

goodness of fit test; it only changes the mean age used to parameterize the cumulative distribution function.

It is likely that factors other than inherited age and sediment reworking contribute to the order-of-magnitude difference in mean age between the radiocarbon ages and the re-scaled distributions (1220 years vs. 118 years and 443 years vs. 55 years). Table 4 shows erosion rates calculated in this study compared with other rates determined in the Oregon Coast Range. In general, the erosion rates calculated in this study are lower than other rates by a factor of two or more. Differences between these rates may be actual or method dependent. For example, the assumption that channel position can be treated as an independent random variable and hence substitute for a random across-valley position may introduce a systematic error. Encroaching tributary debris fans may for example prevent removal of sediment buried within the fan over longer time scales than measured here. However, this effect would tend to skew these distributions to younger ages and hence should provide a greater erosion rate than compared to other methods. Another possibility to explain the low erosion rates calculated by this method is that of greater transient storage. Using the radiocarbon age data to infer erosion rate assumes that most or all of the hillslope material is cycled through the valley floor sediment reservoir and thus is available for radiocarbon dating during the dry season when samples were collected. However, it is likely that the valley floor sediment misses a large portion of the hillslope erosion. For example, Dietrich and Dunne (1978) constructed a sediment budget for Rock Creek in the Oregon Coast Range and estimated that 60 percent of denudation is accomplished through dissolution. This dissolution would leave no sedimentary record within the valley floor and would not be seen in this study's estimate of erosion rates. Although this study's lower estimate of erosion rate includes a weathered rock density, dissolution also removes material from all forms of

sediment both on the hillslopes, in hollows and on the main-stem valley floor. Dietrich and Dunne (1978) also estimated that one-half of soil discharged to channels is carried away as suspended load with the remainder stored in tributaries, debris fans and the floodplain. Incorporation of either of these effects into this study's estimates could increase the actual erosion rate by about a factor of two. Both effects together would increase the erosion rate by about fourfold. Thus, the erosion rates calculated in this study account for only the proportion of the total erosion that forms a deposit on the valley floor such as by debris flows.

Assuming for a moment that the radiocarbon age distribution is not skewed towards older ages, a denudation rate of 0.1 mm/yr as determined by Heimsath et al. (2001) suggests that only 32 and 38 percent of denudation in Bear Creek forms a sedimentary deposit on the valley floor. The remaining 68 and 62 percent of bedrock lowering, then, exits the basin as transient bedload, suspended load and dissolved load. It is likely, however, that the radiocarbon age distribution is skewed toward older ages both by inherited age similar to that determined by Gavin (2001) and by the limitations of radiocarbon dating of sedimentary deposits. Thus, some significant proportion of sediment is missing from the distribution because it moves quickly through the basin and does not form a deposit that is datable by radiocarbon.

Methods	Erosion Rates (mm/yr)	Source
Upper Basin (14C)	0.013 – 0.038	This study
Full Basin (14C)	0.011 – 0.033	This study
Stream Sediment Yields	0.0335	Dietrich and Dunne, 1978
Colluvial Hollows	0.07	Reneau and Dietrich, 1991
Bedrock Exfoliation	0.08	Reneau and Dietrich, 1991
Stream Sediment Yields	0.05 – 0.08	Reneau and Dietrich, 1991
Modeled hillslope transport	0.05 – 0.15	Roering et al., 1999
Soil Production CRNs	0.015 – 0.27	Heimsath et al., 2001
Stream Sediment CRNs	0.11 – 0.12	Heimsath et al., 2001
Stream Sediment CRNs	0.097 – 0.179	Bierman et al., 2001

Table 4. Comparison of erosion rates calculated in Bear Creek with other Oregon Coast Range estimates. CRN = cosmogenic radionuclides.

Valley-Floor Capacitance

The result that the age distribution follows an exponential for the lower reach (0-1300m) supports the hypothesis that this reach of the valley acts as a capacitor to episodic inputs. That is, the storage space provides a buffer for downstream reaches against large but infrequent mass wasting events. Debris flows form sedimentary deposits in this reach but generally do not act to scour the bed or previous deposits. Gradual fluvial processes remove the sediment over time.

The upper reach has mostly young deposits that do not fit an exponential distribution as determined by the KST goodness of fit test. However, the same processes may be operating in the upper reach as the lower reach. Deviations in the shape of upper reach's distribution from exponential may reflect deficiencies in the data related to less sediment stored in the upper reach plus a greater

proportion of sediment that is too young to reliably date by radiocarbon methods. Importantly, the upper reach test fails at repeated zero ages (1950 AD) assigned to the 1996 AD debris flow deposit and post-bomb radiocarbon ages. These ages may represent a span of time up to 50 years. The resolution of radiocarbon dating in determining an age distribution skewed to such younger ages is tenuous at best considering that calibration curves indicate that an age within the last three hundred years could have an actual date anytime between 1650 AD and 1950 AD. Thus, conclusions concerning sediment storage and removal processes in the upper reach cannot be made on the basis of the age distribution alone.

Geomorphic and stratigraphic evidence support the conclusion that the lower reach provides a buffer for downstream reaches against large but infrequent mass wasting events and suggests that such a process may be lacking in the upper reach. For example, the lower reach has more potential sediment storage space relative to the upper valley reach. These two reaches plot as relatively distinct populations on a scatter plot of channel width vs. valley width (Figure 17). Valley width varies over a much wider range than channel width providing more possible channel positions in the valley fill for the lower reach relative to the upper reach. Also the shape of the drainage network varies between the two reaches. The lower reach is relatively straight with tributary junctions at near right angles compared with the upper reach, which is more leaf shaped and has lower-angle tributary junctions (Figure 7). Benda and Cundy (1990) showed bend angle to be important in determining runout length of debris flows when wood was included in the mixture. Importantly, debris flows with much wood (as in the Oregon Coast Range) will stop, i.e. form a deposit, at high-angle junctions and more likely continue through low-angle junctions. Thus debris flow scour is less likely to cause significant bedrock erosion of main-stem lower valley reach relative to the upper reach. Instead, debris flows mainly form deposits in and along the lower reach.

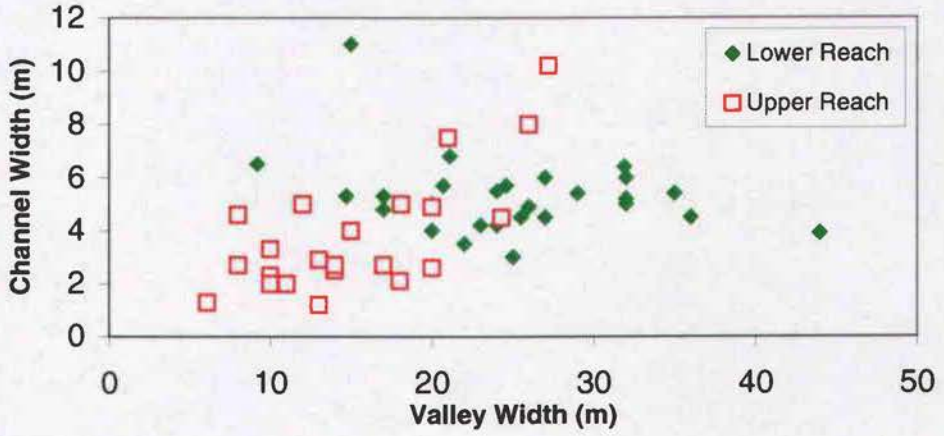

Figure 17. Channel width vs. valley width in Bear Creek. For a given width of channel, the lower basin reach (0-1300 m) has a wider corresponding valley floor available to store sediment away from the channel compared with the upper basin reach (1300-2600 m).

Also revealing are the stratigraphic differences between the lower and upper reaches. Using the randomly chosen points shown in Figures 9, 10, and 11, and Table 1; three definable types of deposits were assigned space in pie charts of thirty points each for the upper and lower reaches weighted by volume (Figure 18). These charts show that the lower basin valley floor exposes an even mix of coarse fluvial gravels, fluvially deposited fines and debris flows. Thus, it appears that fluvial processes dominate sediment transport in the lower reach as represented in the coarse fluvial gravels and fluvially deposited fines. In contrast, the upper-reach storage is composed almost entirely of debris flow deposits, a fact that suggests that much of the geomorphic work here is done by debris-flow scour with lesser amounts of fluvial transport and erosion. In the upper-most section of the upper reach, the main channel resembles a bedrock chute with little or no sedimentary deposits characteristic of a debris-flow—carved channel. The young deposits in the narrower valley reaches have a greater likelihood that they will be scoured out by larger debris flows and debris flow scour may also be the dominant process of bedrock channel erosion.

Future study may validate these conclusions. Important directions for study include modeling efforts that attempt to address what sets the size of the accommodation space for sediment storage including the interactions between sediment supply and removal, lateral and vertical bedrock erosion and other factors such as contributing area and channel slope. Also, independent measures of erosion rates in the basin by methods such as cosmogenic radionuclide concentrations in stream sediments (e.g. Granger et al., 1996; Bierman and Steig, 1996; Riebe et al., 2000; Riebe et al., 2001; Riebe et al., 2003; Kirchner et al. 2001; Brown et al., 1995) will also better constrain the role of the valley storage in the sediment budget.

Figure 18. Comparison of the relative stratigraphy of the lower reach (0-1300 m) and the upper reach (1300-2600m). Each chart includes 30 points listed in table 1. DF = Debris flow deposit, FF = Fluvially deposited fines, FG = Coarse fluvial gravel.

CONCLUSIONS

In this study, radiocarbon dating was used to determine the residence time and mean age of the valley floor sediment in Bear Creek. These ages combined with sediment volume surveys were then used to calculate basin average erosion rates of 0.011 – 0.033 and 0.013 – 0.038 mm/yr. Erosion rates thus calculated are lower than erosion rates calculated for other study sites within the Oregon Coast Range. This possible discrepancy may be real or may reflect method error. A real difference cannot be ruled out without separate measures of erosion rates, but method errors are identifiable. Important sources of error include inherited age of radiocarbon samples. Also important processes are denudation of hillslopes by dissolution, and sediment transport by suspended load and transient bedload that does not form a valley floor sedimentary deposit. By comparing the erosion rates calculated with higher erosion rates as determined by other studies in the OCR, it appears that the valley storage acts as a capacitor to as little as ~25 percent of the sediment supply (assuming dissolution accounts for ~60 percent of the denudation). This suggests that as much as ~75 percent of the sediment supply (~90 percent of the denudation) flushes through the basin with little attenuation.

The age distributions for the upper and lower basin reaches were used to determine whether or not the valley floor acts as a capacitor to episodic mass wasting events. Statistical analysis suggest that the lower reach of Bear Creek acts as a buffer for the sediment supply while the upper reach may or may not. These conclusions are supported by geomorphic and stratigraphic evidence. The lower basin valley floor sediment is a mixture of debris flow and fluvial deposits while the upper basin valley floor sediment is composed almost entirely of debris flow deposits. Also, the lower basin has a wide valley floor relative to the channel width that provides storage space for sediment. The upper basin has a narrower valley floor with less space for sediment storage. Thus, debris flows predominately form deposits in the lower reach that are then removed by fluvial

processes. Deviations in the shape of upper reach's distribution from exponential may be due to lesser sediment storage in the upper reach plus a greater proportion of sediment that is too young to reliably date by radiocarbon methods. Future directions for research include modeling efforts to determine the factors influencing the valley widths as well as independent measures of erosion rates by the method using cosmogenic radionuclide concentrations in stream sediments.

BIBLIOGRAPHY

Anderson, S. P., W. E. Dietrich, and G. H. Brimhall Jr., Weathering profiles, mass-balance analysis, and rates of solute loss: Linkages between weathering and erosion in a small, steep catchment, *GSA Bulletin, 114*, 1143-1185, 2002.

Benda, L. E., and T. W. Cundy, Predicting deposition of debris flows in mountain channels, *Can. Geotech. J., 27*(4), 409-417, 1990.

Benda, L., and T. Dunne, Stochastic forcing of sediment supply to channel networks from landsliding and debris flow, *Water Resour. Res., 33,* 2849-2863, 1997a.

Benda, L., and T. Dunne, Stochastic forcing of sediment routing and storage in channel networks, *Water Resour. Res. 33,* 2865-2880, 1997b.

Benjamin, J. R., and C. A. Cornell, *Probability, Statistics, and Decision for Civil Engineers,* 684 pp., McGraw-Hill, New York, 1970.

Bierman, P., and E. J. Steig, Estimating rates of denudation using cosmogenic isotope abundances in sediment, *Earth Surf. Process Landforms, 21,* 125-139, 1996.

Bierman, P., E. Clapp, K. Nichols, A. Gilespie, and M. W. Caffee, Using cosmogenic nuclide measurements in sediments to understand background rates of erosion and sediment transport, *Landscape Erosion and Evolution Modeling,* edited by R. S. Harmon and W. W. Doe III, pp. 89-115, Kluwer Academic/Plenum Publishers, New York, 2001.

Brown, E. T., R. F. Stallard, M. C. Larsen, G. M. Raisbeck, and F. Yiou, Denudation rates determined from the accumulation of in-situ produced ^{10}Be in the Luquillo Experimental Forest, Puerto Rico, *Earth Plan. Sci. Letters, 129,* 193-202, 1995.

Dietrich, W. E., and T. Dunne, Sediment budget for a small catchment in mountainous terrain, *Z. Geomorphol. Suppl., 29,* 191-206, 1978.

Drake, A. W., *Fundamentals of Applied Probability Theory,* McGraw-Hill Book company, New York, 283 pp., 1967.

Granger, D. E., J. W. Kirchner, and R. Finkel, Spatially averaged long-term erosion rates measured from in situ-produced cosmogenic nuclides in alluvial sediment, *J. Geol., 104,* 249-257, 1996.

Harleman, D. R. F., *Transport Processes in Environmental Engineering*, (A series of notes to accompany lectures in 1.77 Water Quality Control),

Massachusetts Institute of Technology, Cambridge, irregular pagination, 1990.

Hancock, G. S., and R. S. Anderson, Numerical modeling of fluvial strath-terrace formation in response to oscillating climate, *GSA Bulletin, 114*, 1131-1142, 2002.

Heimsath, A. J., W. E. Dietrich, K. Nishizumi, and R. C. Finkel, Stochastic processes of soil production and transport: erosion rates, topographic variation and cosmogenic nuclides in the Oregon Coast Range, *Earth Surf. Process Landforms, 26,* 531-552, 2001.

Iverson, R. M., M. E. Reid, and R. G. LaHusen, Debris-flow mobilization from landslides, *Annu. Rev. Earth Planet. Sci. 25,* 85-138,1997.

Iverson, R. M., M. E. Reid, N. R. Iverson, R. G. LaHusen, M. Logan, J. E. Mann, and D. L. Brien, Acute sensitivity of landslide rates to initial soil porosity, *Science, 290*(5491), 513-516, 2000.

Kirchner, J. W., R. C. Finkel, C. S.Riebe, D. E. Granger, J. L. Clayton, J. G. King, and W. F. Megahan, Mountain erosion over 10 yr, 10 k.y., and 10 m.y. time scales, *Geology, 29*, 591-594, 2001.

Khamis, H. J., The two-stage δ-corrected Komogorov-Smirnov test, *J. Applied Statistics, 27,* 439-4500, 2000.

Lancaster, S. T., S. K. Hayes and G. E. Grant, Modeling Sediment and Wood Storage Dynamics in Small Mountainous Watersheds, *Geomorphic Processes and Riverine Habitat,* edited by J. M. Dorava, D. R. Montgomery, B. B. Palcsak, and F. A. Fitzpatrick, pp. 85-102, American Geophysical Union, Washington, 2001.

Lancaster, S.T., S.K. Hayes, and G.E. Grant, Effects of wood on debris flow runout in small mountain watersheds, *Water Resour. Res., 39*(6), 1168, doi:10.1029/2001WR001227, 2003.

Levenspiel, O., andK. B. Bischoff, Patterns of flow in chemical process vessels, *Adv. Chem. Eng.,* 4, 56, 1963 (cited in Harleman, 1990)

Lisle, T. E. and M. Church, Sediment transport-storage relations for degrading, gravel bed channels, *Water Resour. Res., 38*(11), 1219, doi:10.1029/2001WR001086, 2002.

Meyer, G. A., S. G., Wells, and A. J. T. Jull, Fire and alluvial chronology in Yellowstone National Park: Climatic and intrinsic controls on Holocene geomorphic processes, *GSA Bulletin, 107,* 1211-1230, 1995.

Miller, D. J., and L. E. Benda, Effects of punctuated sediment supply on valley-floor landforms and sediment transport, *GSA Bulletin, 112,* 1814-1824, 2000.

Montgomery, D. R., T. M. Massong, and S. C. S. Hawley. Influence of debris flows and log jams on the location of pools and alluvial channel reaches, Oregon Coast Range, *GSA Bulletin, 115,* 78-88, 2003.

Oregon Climate Service, Monthly means and extremes, Honeyman State Park, Oregon, 1971-1990, Corvallis, 1990. (Available at http://www.ocs.orst.edu/pub_ftp/climate_data/mme/mme3995.html)

Personius, S. F., H. M. Kelsey, and P. C. Grabau, Evidence for regional stream aggradation in the Central Oregon Coast Range during the Pleistocene-Holocene transition, *Quaternary Res., 40,* 297-308, 1993.

Ramsey, B., 2003, OxCal Version 3.9: Oxford, UK, University of Oxford, downloaded in July 2004, available from http://www.rlaha.ox.ac.uk/orau/oxcal.html.

Reid, M. E., R. G. LaHusen, and R. M. Iverson, Debris-flow initiration experiments using diverse hydrologic triggers, in *Debris-flow Hazards Mitigation: Mechanicx Prediction and Assessment,* edited by C. L. Chen, pp. 1-11, A.S.C.E., New York, 1997.

Reneau, S. L., and W. E. Dietrich, Erosion rates in the Southern Oregon Coast Range: Evidence for an equilibrium between hillslope erosion and sediment yield, *Earth Surf. Processes Landforms, 16,* 307-322, 1991.

Reneau, S. L., W. E. Dietrich, M. Rubin, D. J. Donahue, and A. J. T. Jull, Analysis of hillslope erosion rates using dated colluvial deposits, *J. Geol., 97,* 45-63, 1989.

Richards, K., Drainage basin structure, sediment delivery and the response to environmental change, *Sediment Flux to Basins: Causes, Controls and Consequences,* edited by S. J. Jones and L. E. Frostick, pp. 149-160, Geological Society, London, Special Publications, 191, 2002.

Riebe, C. S., J. W. Kirchner, D. E. Granger, R. C. Finkel, Erosional equilibrium and disequilibrium in the Sierra Nevada, inferred from cosmogenic ^{26}Al and ^{10}Be in alluvial sediment, *Geology, 28,* 803-806, 2000.

Riebe, C. S., J. W. Kirchner, D. E. Granger, R. C. Finkel, Minimal climatic control on erosion rates in the Sierra Nevada, California, *Geology, 29,* 447-450, 2001.

Riebe, C. S., J. W. Kirchner, and R. C. Finkel, Long-term rates of chemical weathering and physical erosion from cosmogenic nuclides and

geochemical mass balance, *Geochem. Cosmochimica Acta., 67,* 4411-4427, 2003.

Roering, J. J., J. W. Kirchner, and W. E. Dietrich, Evidence for nonlinear diffusive sediment transport on hillslopes and implications for landscape morphology, *Water Resour. Res., 35*, 853-870, 1999.

Roering, J. J., J. W. Kirchner, and W. E. Dietrich, Characterizing structural and lithologic controls on deep-seated landsliding: Implications for topographic relief and landscape evolution in the Oregon Coast Range, USA, *GSA Bulletin*, in press.

Sklar, L. and W. E. Dietrich, River longitudinal profiles and bedrock incision models: Stream power and the influence of sediment supply, in *Rivers Over Rock: Fluvial Processes in Bedrock Channels, Geophys. Monogr. Ser.,* v. 107, edited by K. J. Tinkler and E. E. Wohl, pp. 237-260, AGU, Washington, D. C., 1998.

Sklar, L. S. and W. E. Dietrich, Sediment and rock strength controls on river incision into bedrock, *Geology, 29,* 1087-1090, 2001.

Stock, J. and W. E. Dietrich, Valley incision by debris flows: Evidence of a topographic signature, *Water Resour. Res., 39,* 1089, doi:1029/2001WR001057, 2003.

Tucker, G. E., and R. L. Bras, Hillslope processes, drainage density, and landscape morphology, *Water Resour. Res., 36,* 2751-2764, 1998.

Wegmann, K. W., and F. J. Pazzaglia, Holocene strath terraces, climate change, and active tectonics: The Clearwater River basin, Olympic Peninsula, Washington State, *GSA Bulletin, 114,* 731-744, 2002.

Whipple, K. X., and G. E. Tucker, Implications of sediment-flux-dependent river incision models for landscape evolution, *J. Geophys. Res.,107*(B2), 20pp., 2002.